One-dimensional Kinetic Simulation of Parametric Instabilities in Strongly Magnetized Electron-Positron Plasma

Shoma Kamijima (YITP, Kyoto U.)

Collaborators: Masanori Iwamoto (YITP, Kyoto U.), Rei Nishiura (Kyoto U.), Wataru Ishizaki (Tohoku U.), Kunihito Ioka (YITP, Kyoto U.)

Fast Radio Burst (FRB)

- Most luminous radio transient
- Large dispersion measure
  →Cosmological
- Frequency: $\nu \sim \mathcal{O}(\mathrm{GHz})$
- Duration: $\Delta t \sim \mathcal{O}(\mathrm{msec})$
- Flux density: $S_\nu \sim \mathcal{O}(\mathrm{Jy})$ @GHz
- High Brightness temperature:
  → Coherent emission
- FRB from Galactic magnetar
  is observed in 2020.

One of the origins of FRBs is a magnetar.

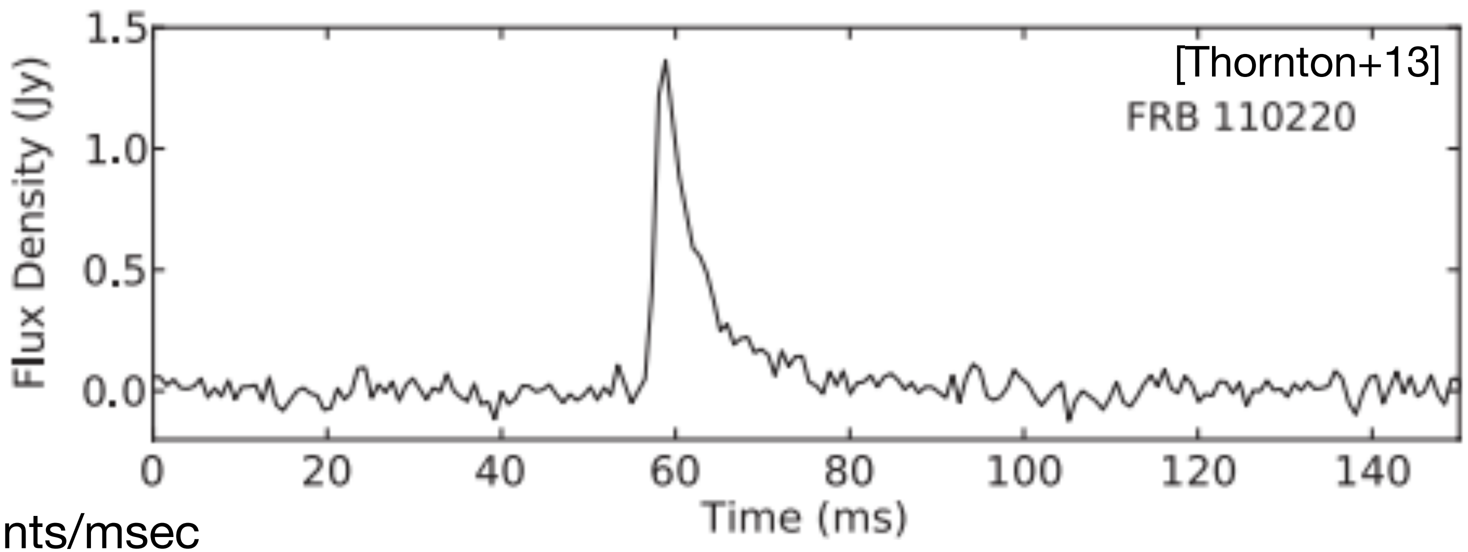

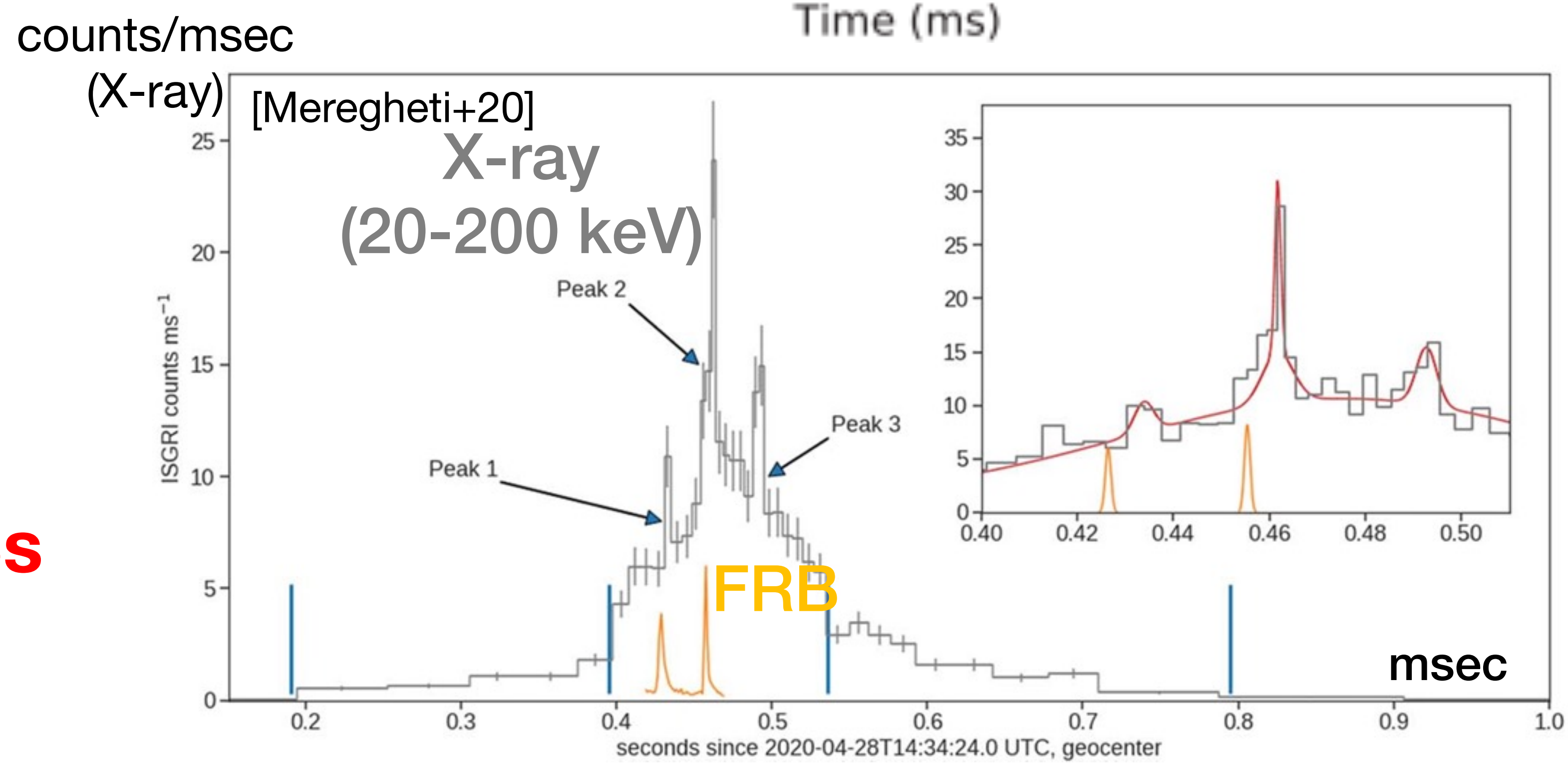

Magnetar Model

The wave propagation in magnetized plasma is common for both models.
Parametric instabilities are important for wave propagation in plasma.

Inner Magnetosphere Model

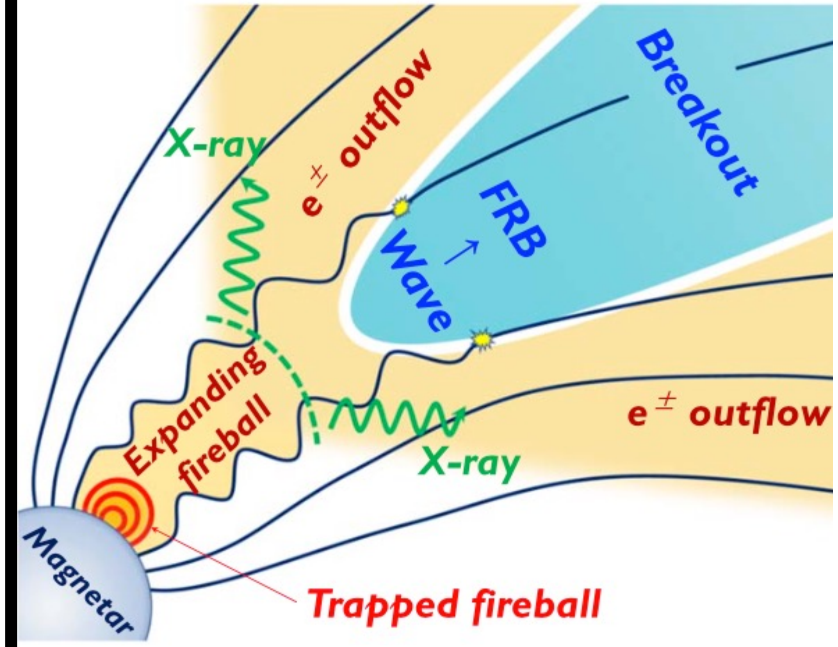

[Ioka 2020]

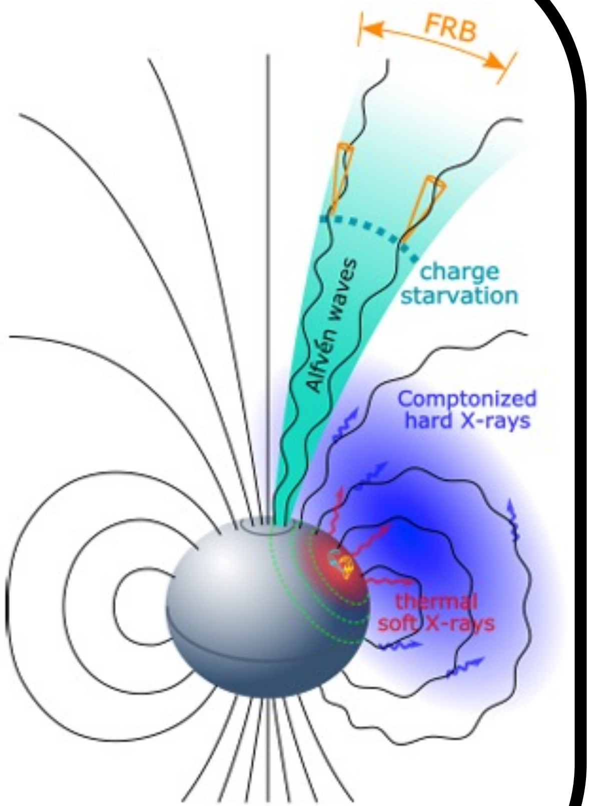

[Lu+2020]

Outer Magnetosphere Model

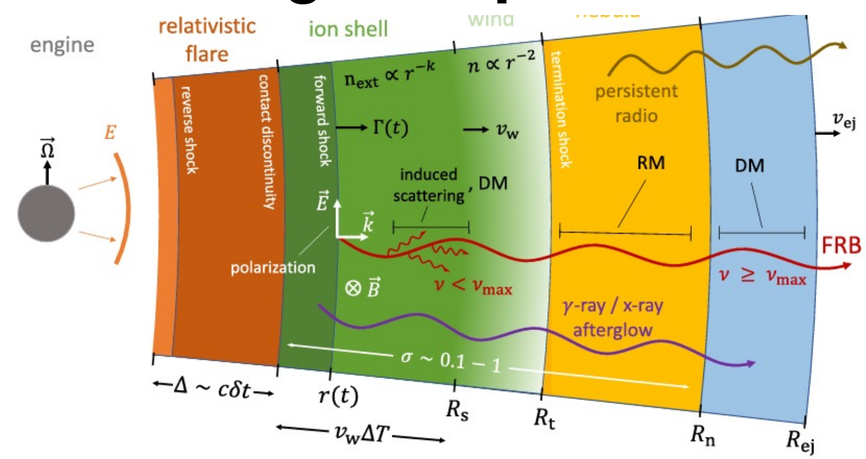

[Metzger+2019]

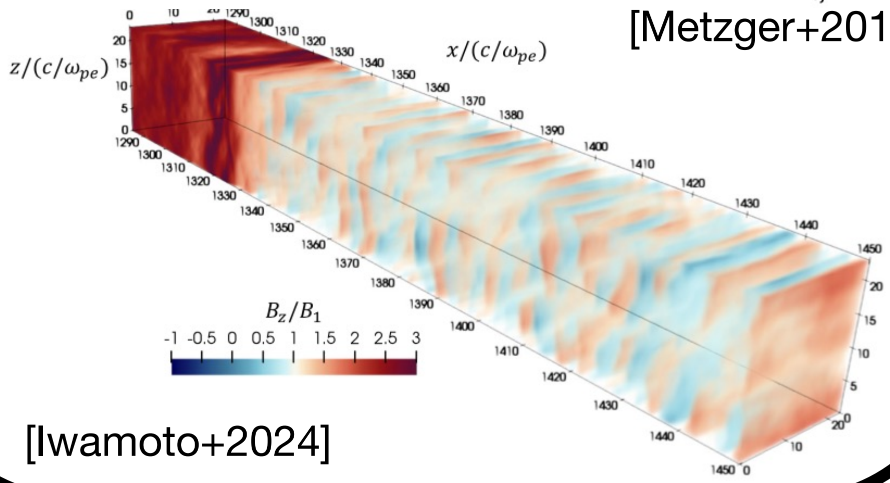

[Iwamoto+2024]

Parametric Instability in Unmagnetized Plasma

Particles oscillated by the incident wave make the nonlinear current.

The nonlinear current generates the scattered wave.

The beating wave between the incident and scattered waves is created.

The ponderomotive force acts on particles.

The density fluctuation is amplified.

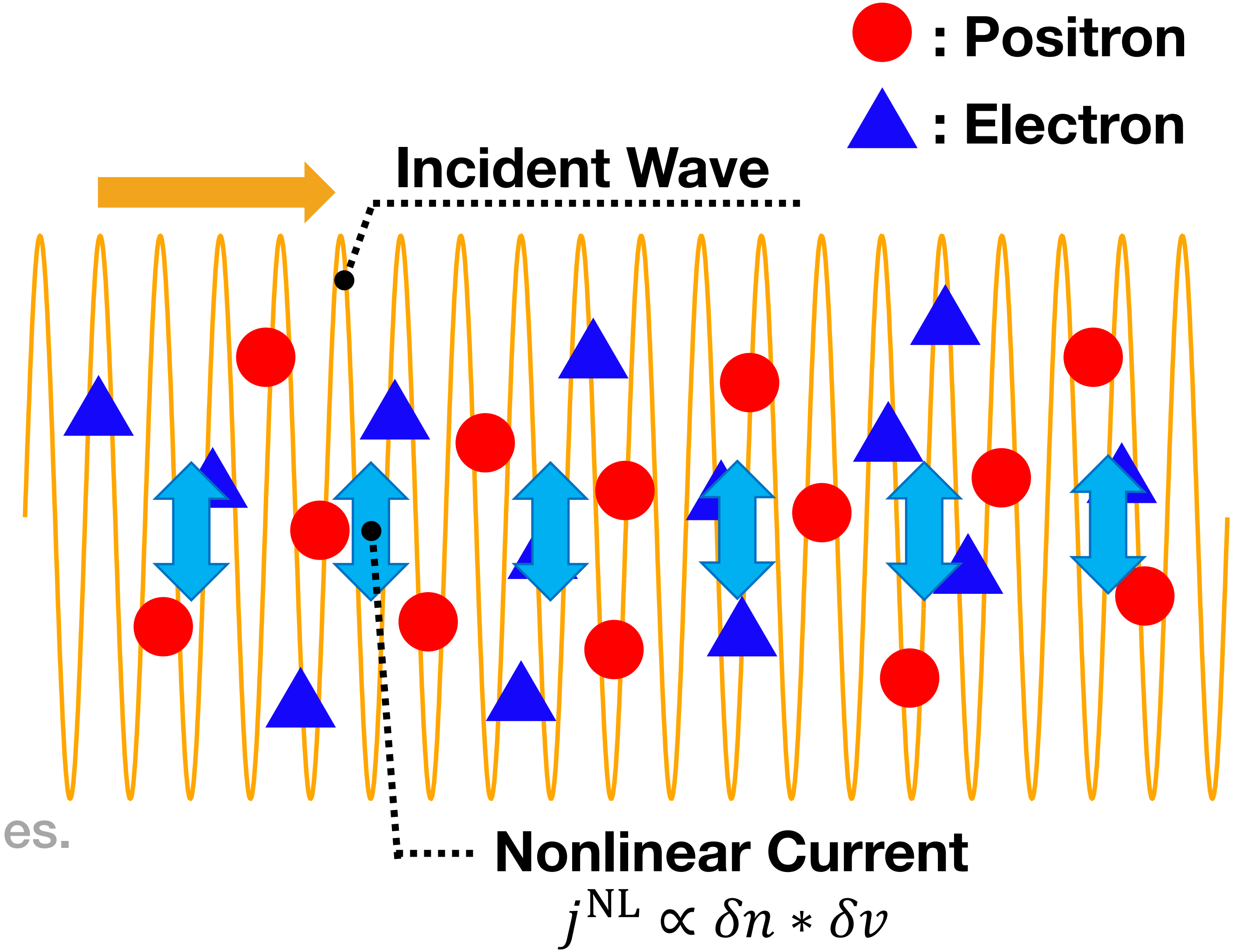

Parametric Instability in Unmagnetized Plasma

Particles oscillated by the incident wave make the nonlinear current.

The nonlinear current generates the scattered wave.

The beating wave between the incident and scattered waves is created.

The ponderomotive force acts on particles.

The density fluctuation is amplified.

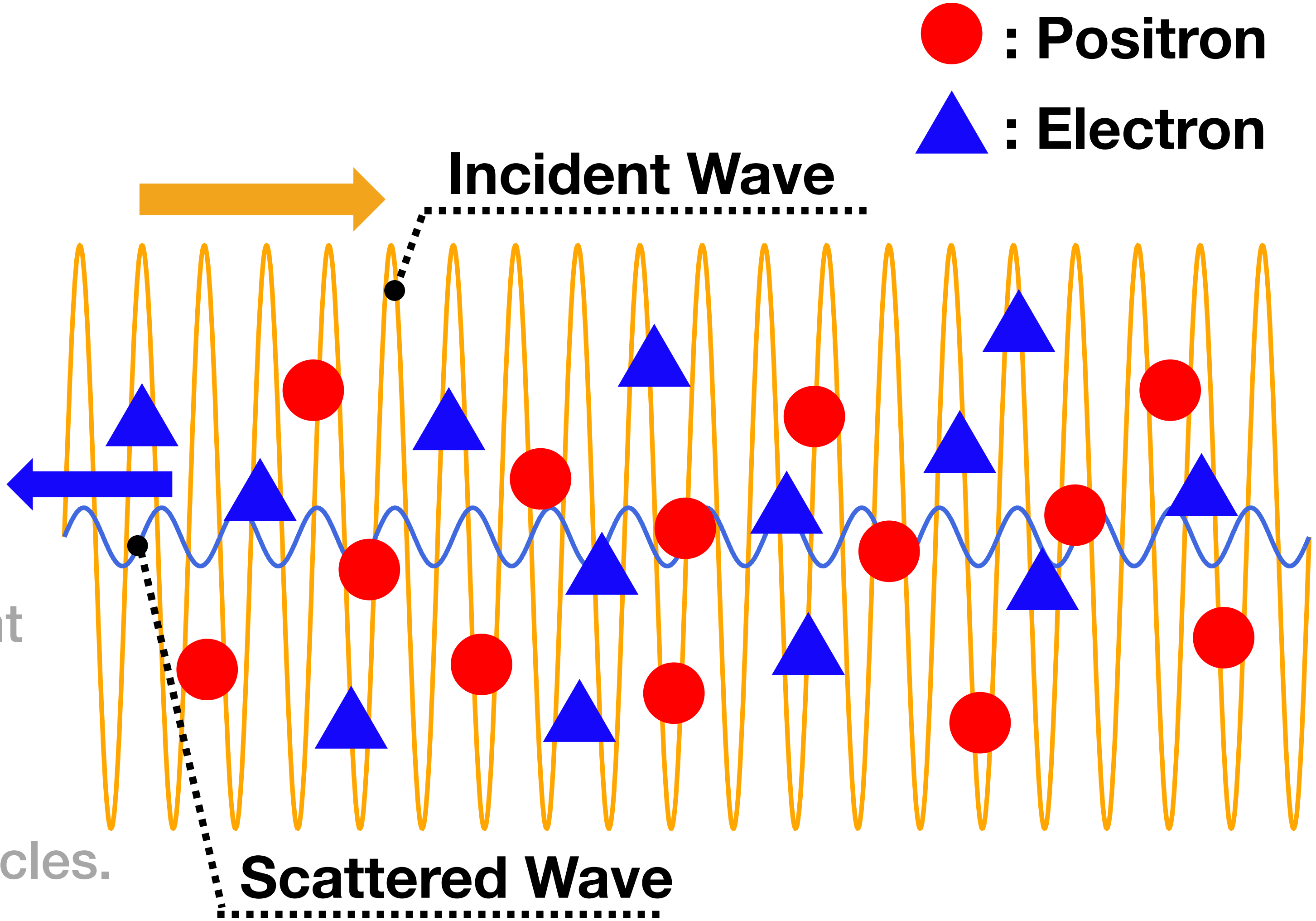

Parametric Instability in Unmagnetized Plasma

Particles oscillated by the incident wave make the nonlinear current.

The nonlinear current generates the scattered wave.

The beating wave between the incident and scattered waves is created.

The ponderomotive force acts on particles.

The density fluctuation is amplified.

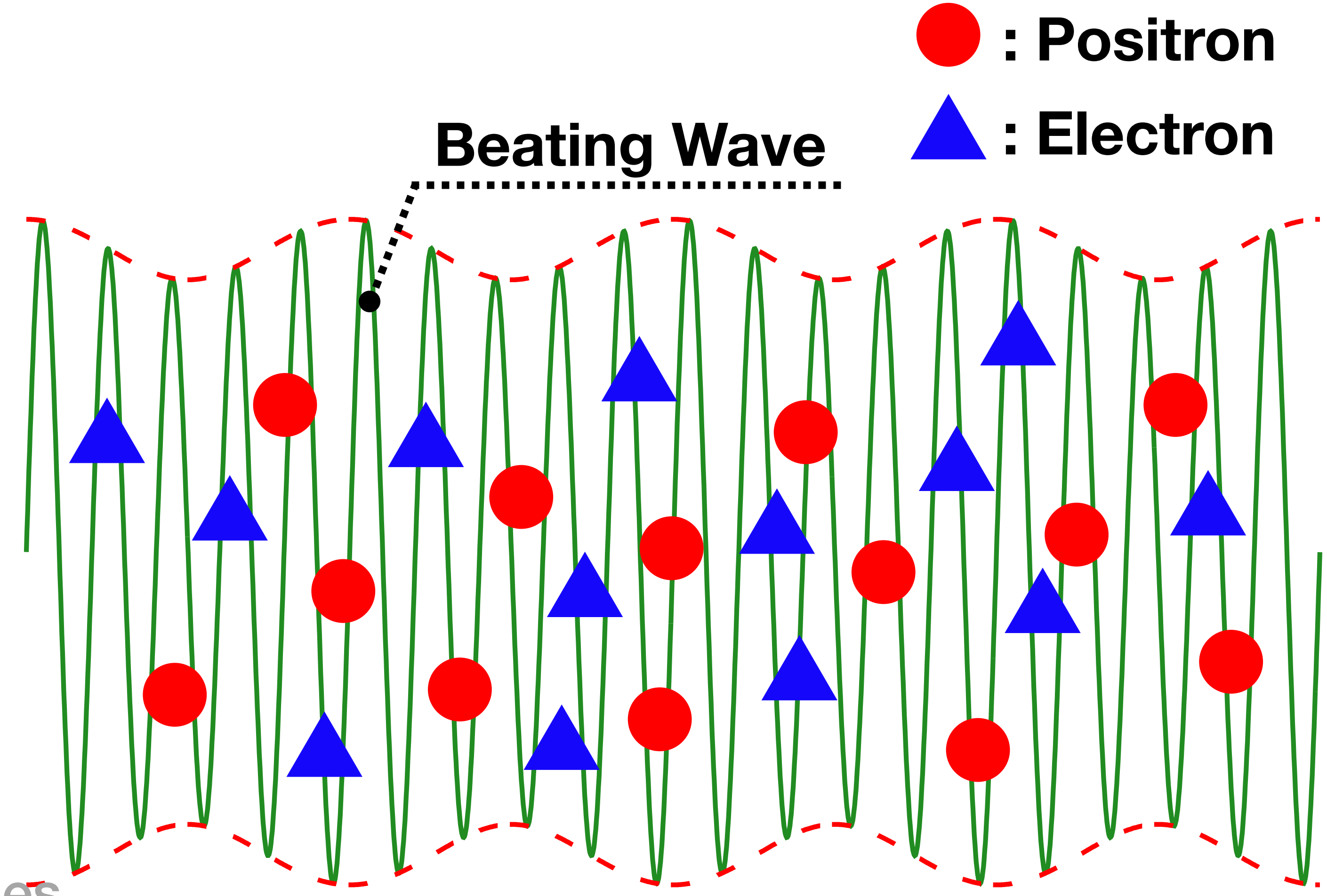

Parametric Instability in Unmagnetized Plasma

Particles oscillated by the incident wave make the nonlinear current.

The nonlinear current generates the scattered wave.

The beating wave between the incident and scattered waves is created.

The ponderomotive force acts on particles.

The density fluctuation is amplified.

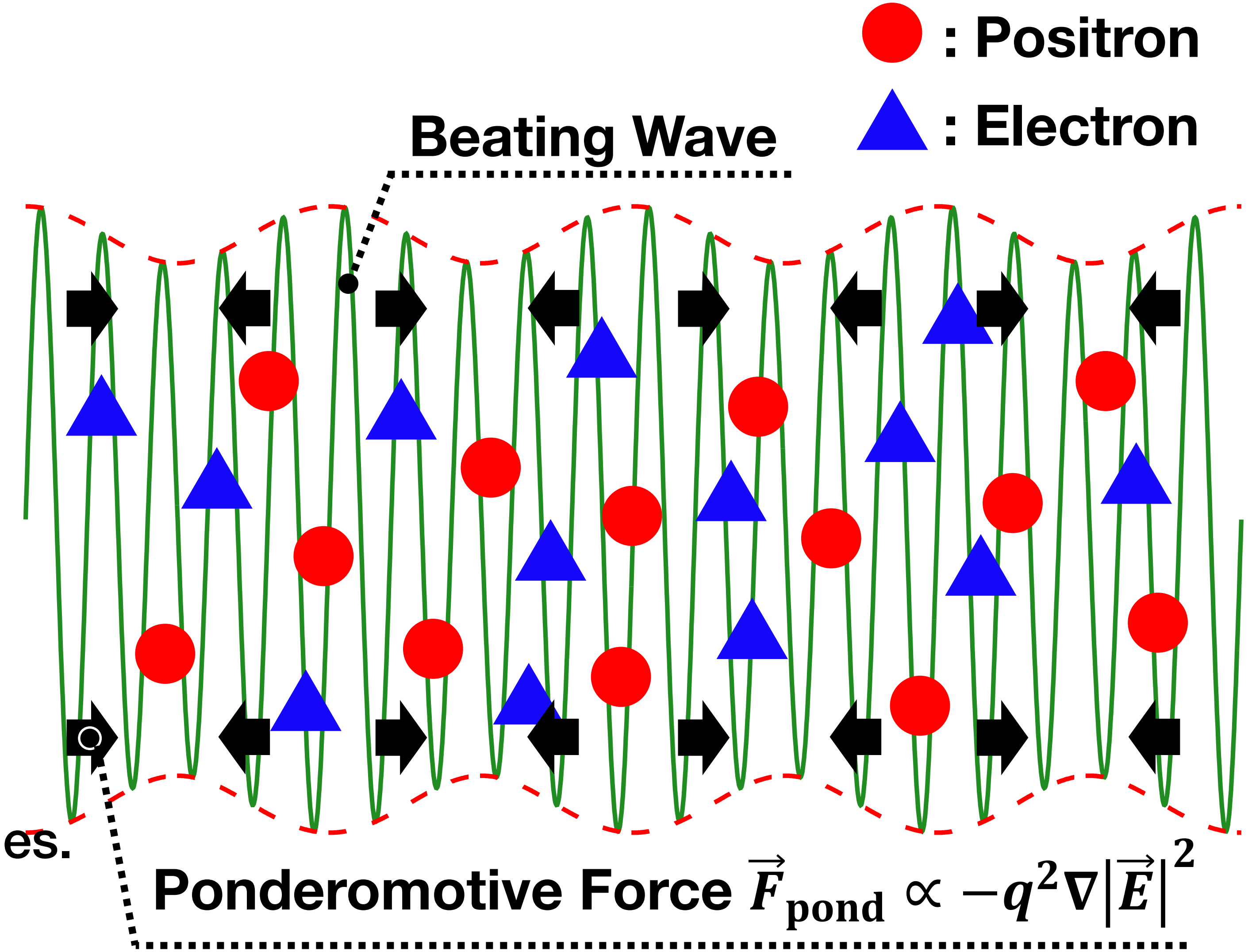

Parametric Instability in Unmagnetized Plasma

Particles oscillated by the incident wave make the nonlinear current.

The nonlinear current generates the scattered wave.

The beating wave between the incident and scattered waves is created.

The ponderomotive force acts on particles.

The density fluctuation is amplified.

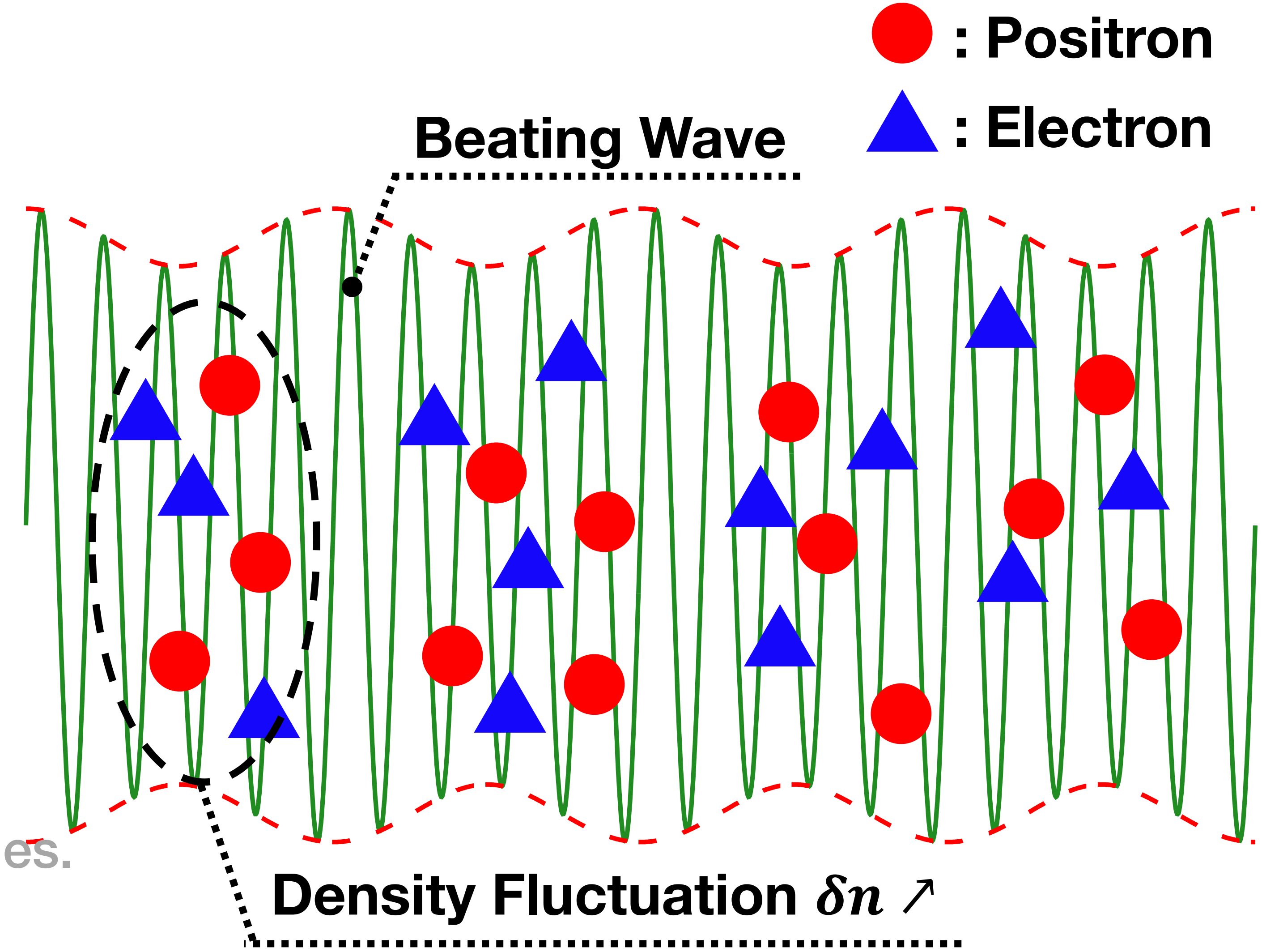

Parametric Instability in Unmagnetized Plasma

Particles oscillated by the incident wave make the nonlinear current.

The nonlinear current generates the scattered wave.

The beating wave between the incident and scattered waves is created.

The ponderomotive force acts on particles.

The density fluctuation is amplified.

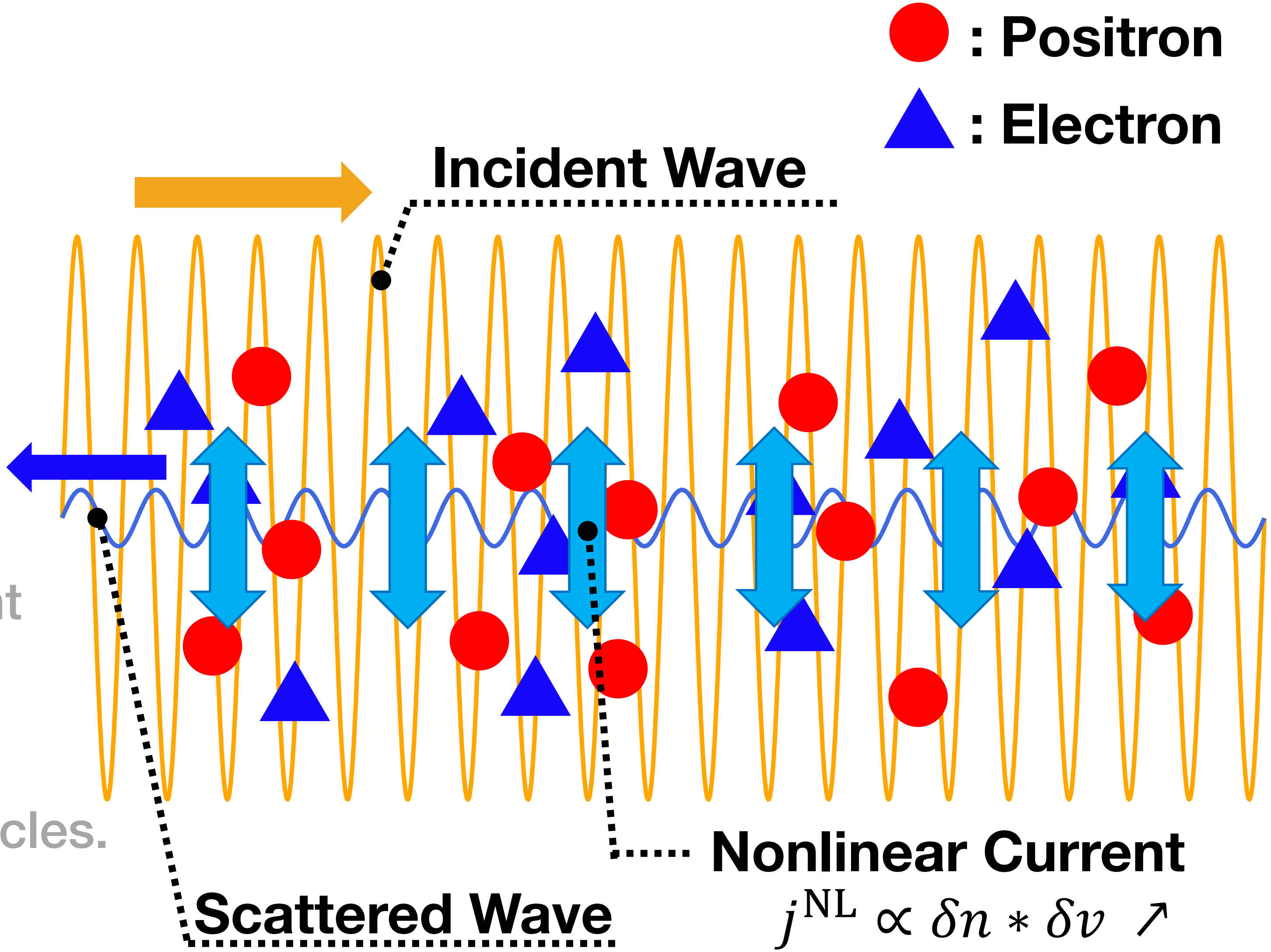

Parametric Instability in Unmagnetized Plasma

Particles oscillated by the incident wave make the nonlinear current.

The nonlinear current generates the scattered wave.

The beating wave between the incident and scattered waves is created.

The ponderomotive force acts on particles.

The density fluctuation is amplified.

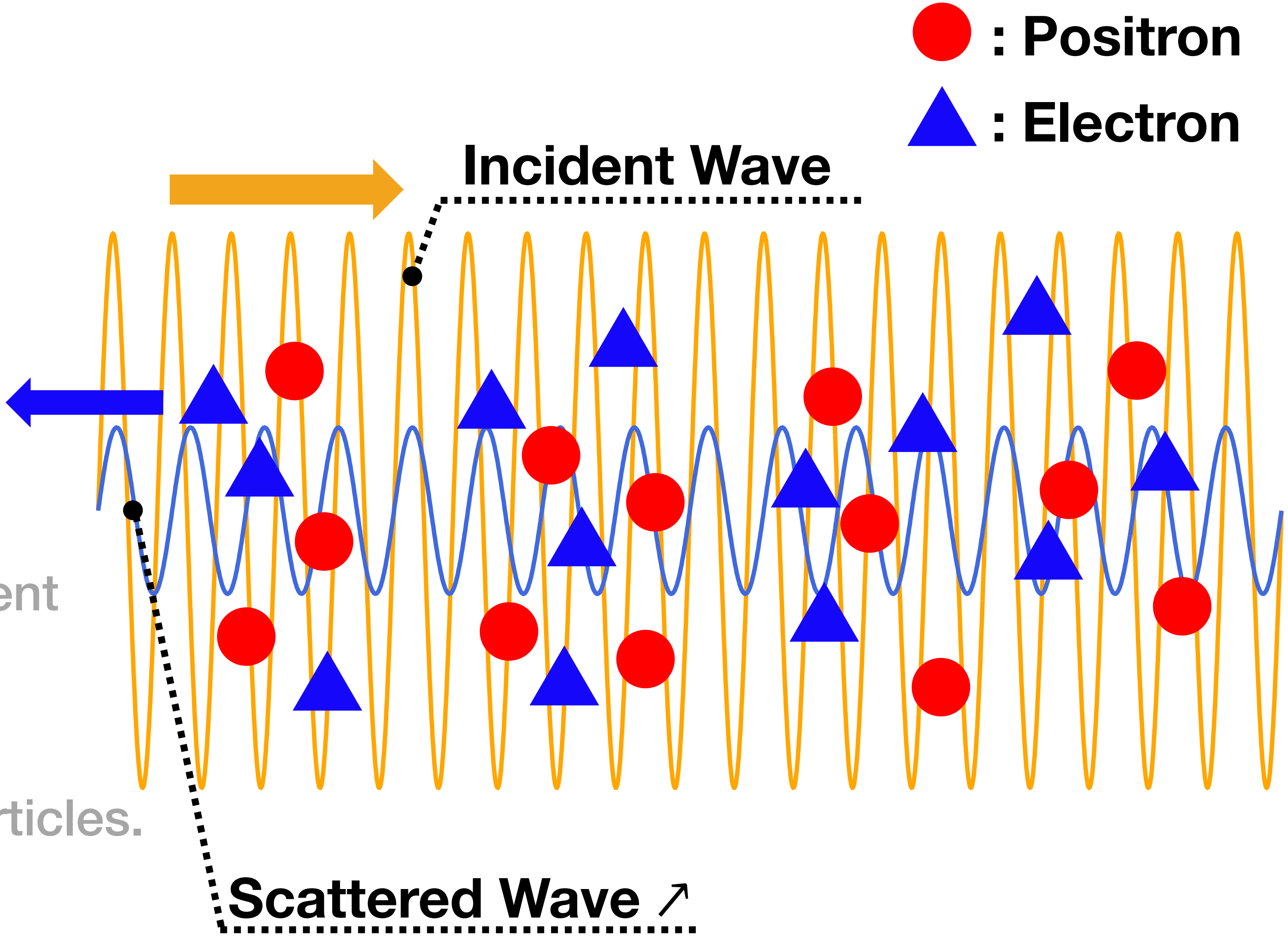

Parametric Instability in Unmagnetized Plasma

Particles oscillated by the incident wave make the nonlinear current.

The nonlinear current generates the scattered wave.

The beating wave between the incident and scattered waves is created.

The ponderomotive force acts on particles.

The density fluctuation is amplified.

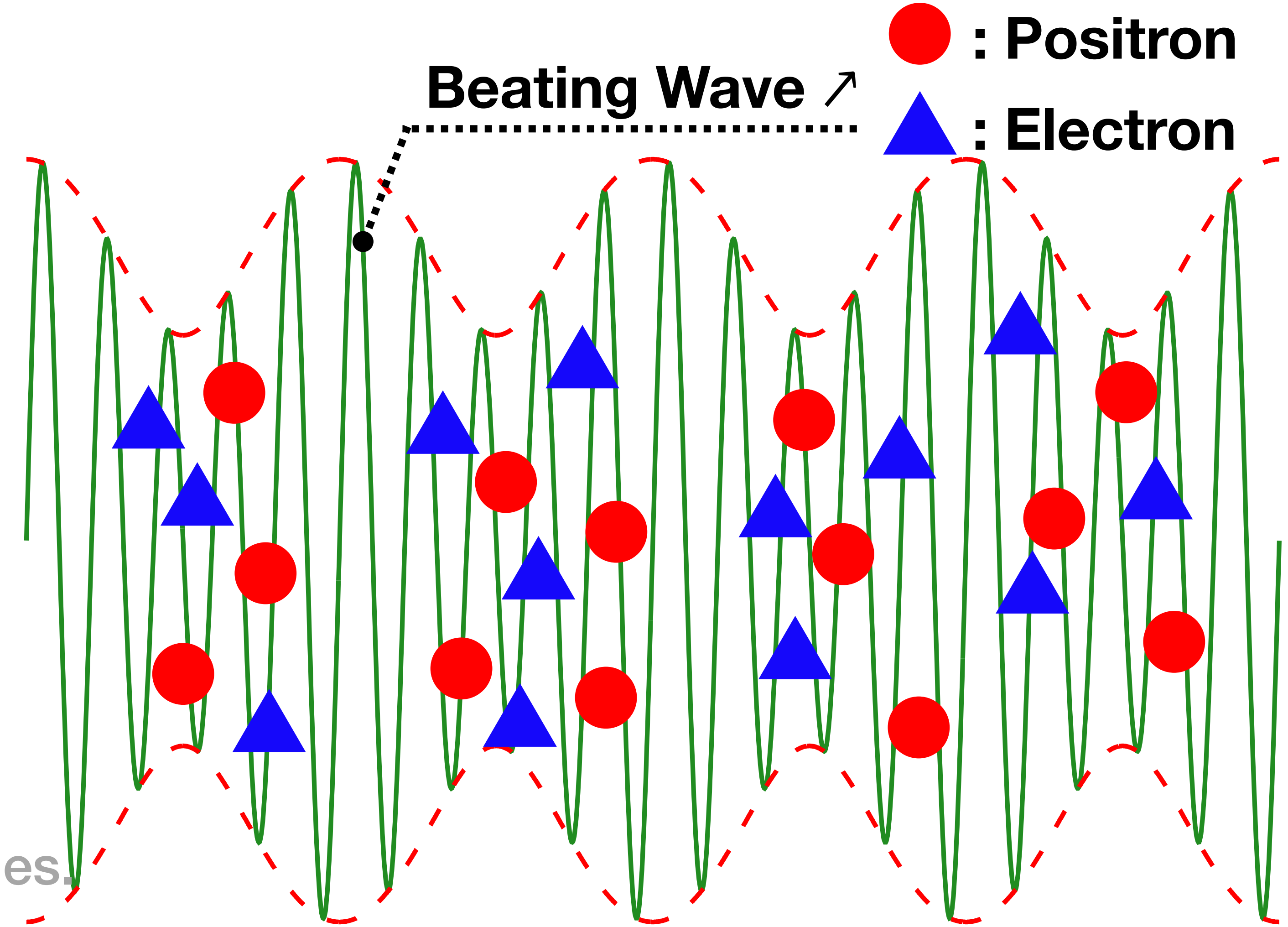

Parametric Instability in Unmagnetized Plasma

Particles oscillated by the incident wave make the nonlinear current.

The nonlinear current generates the scattered wave.

The beating wave between the incident and scattered waves is created.

The ponderomotive force acts on particles.

The density fluctuation is amplified.

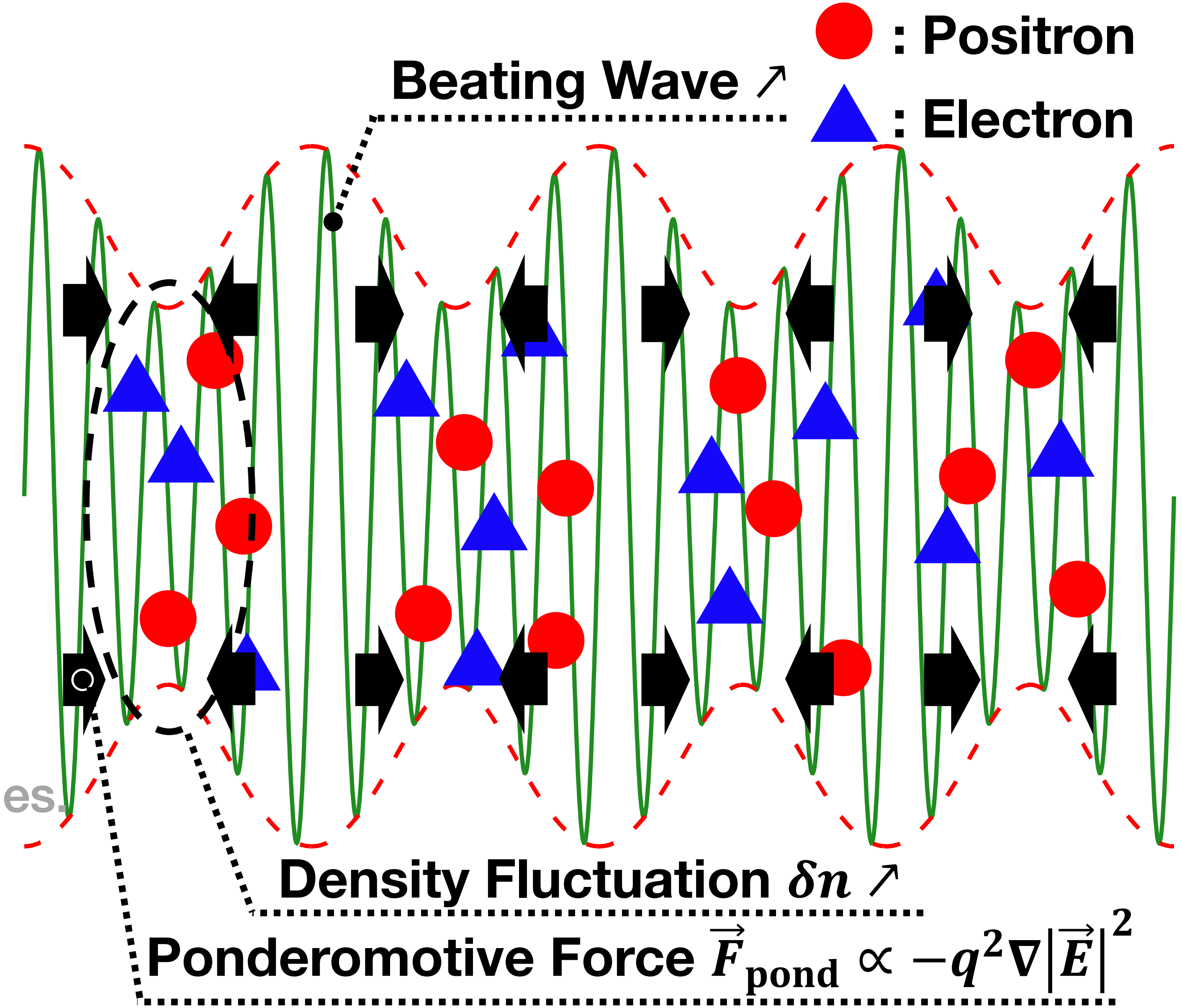

Parametric Instability

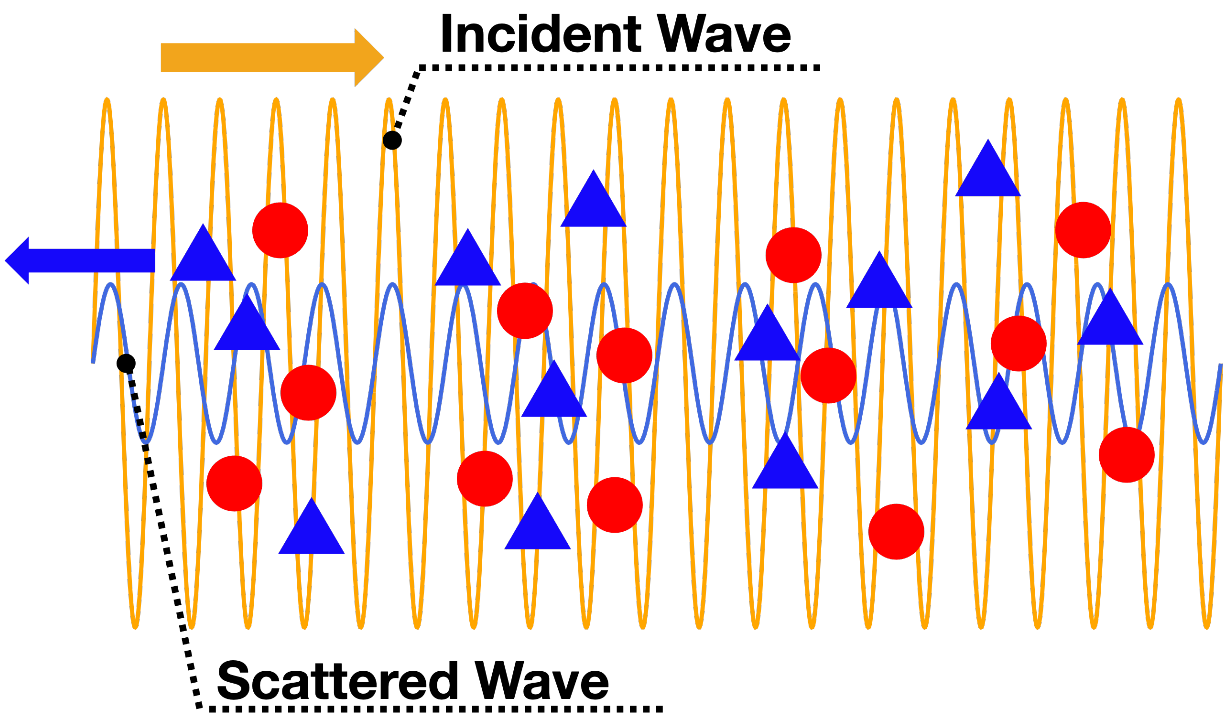

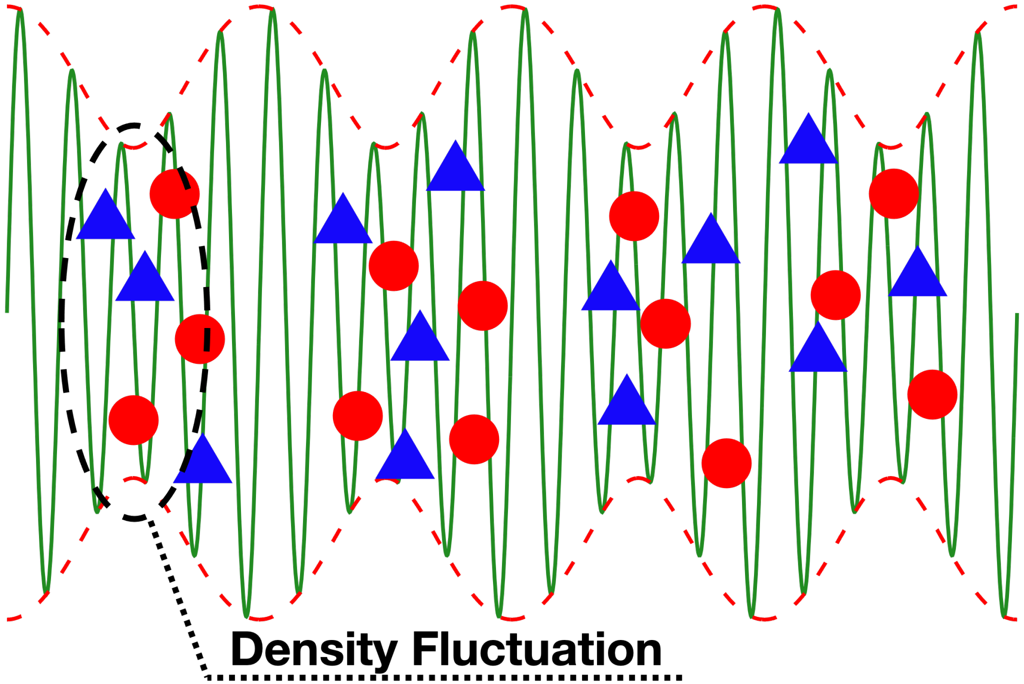

Incident wave	→	Scattered wave	+	Density fluctuation
(Transverse mode)		(Transverse mode)		(Longitudinal mode)

$$\begin{pmatrix}\omega_0\\ k_0\end{pmatrix} = \begin{pmatrix}\omega_1\\ k_1\end{pmatrix} + \begin{pmatrix}\omega\\ k\end{pmatrix}$$

Incident waves lose their energy while propagating in plasma.

Parametric Instability for FRB

☐ Escape of waves from the magnetar magnetosphere/wind

Induced Compton scatterings (ICS) prevent from propagation of FRB emission and Alfvén wave.

☐ Growth rate of ICS **w/o background B-field** [Drake+1974, Ghosh+2022]

$$\Gamma_{\rm c,max}^{{\rm w/o}\,B} = \sqrt{\frac{\pi}{32{\rm e}}}\frac{\omega_{\rm p}^2 a_{\rm e}^2}{\omega_0}\frac{m_{\rm e}c^2}{k_{\rm B}T_{\rm e}} \sim 10^{20}\ {\rm sec}^{-1}\,\frac{B_{\rm p,14}\mathcal{M}_6 L_{38} R_{\rm NS,6}}{P_{\rm sec} r_8^5 v_9^3 T_{80\,{\rm keV}}} \gg t_{\rm dyn}^{-1}$$

$$t_{\rm dyn}^{-1} = \frac{c}{r} \sim 3.0\times 10^2\ {\rm sec}^{-1}\ r_8^{-1}$$

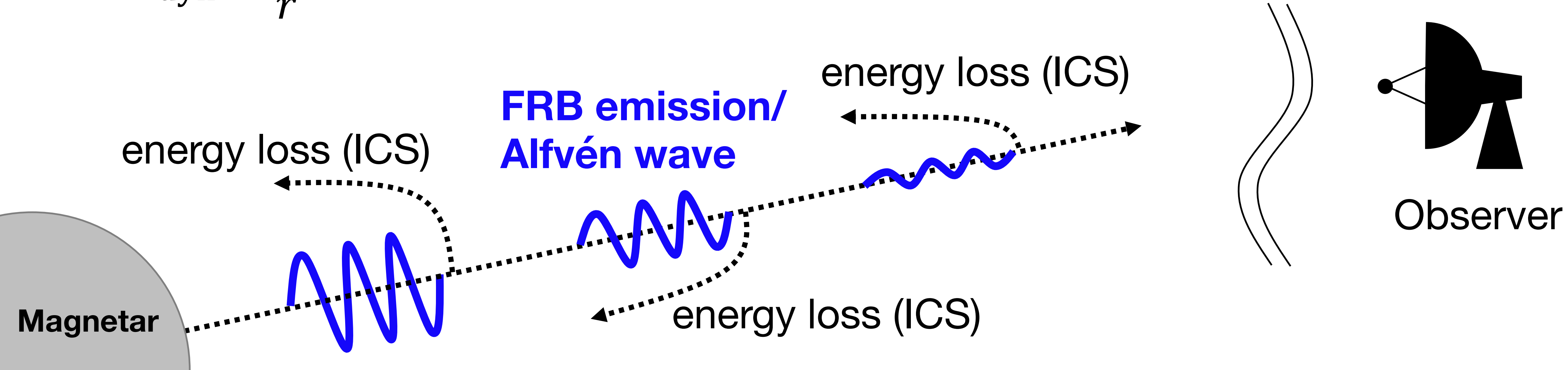

Growth Rate of ICS in Magnetized Plasma

The background B-field suppresses the growth rate of ICS.

$$\Gamma_{\rm c,max}^{{\rm w/}\,B} = \Gamma_{\rm c,max}^{{\rm w/o}\,B} \times \left[O\left(\frac{\omega_0}{\omega_c}\right)^2 + O\left(\frac{\omega_0}{\omega_c}\right)^4 \right]$$

$\omega_{\rm c} = eB_0/(m_e c)$:cyclotron freq.
$> \omega_0$:incident wave freq.

[e.g. Nishiura & Ioka 2024]

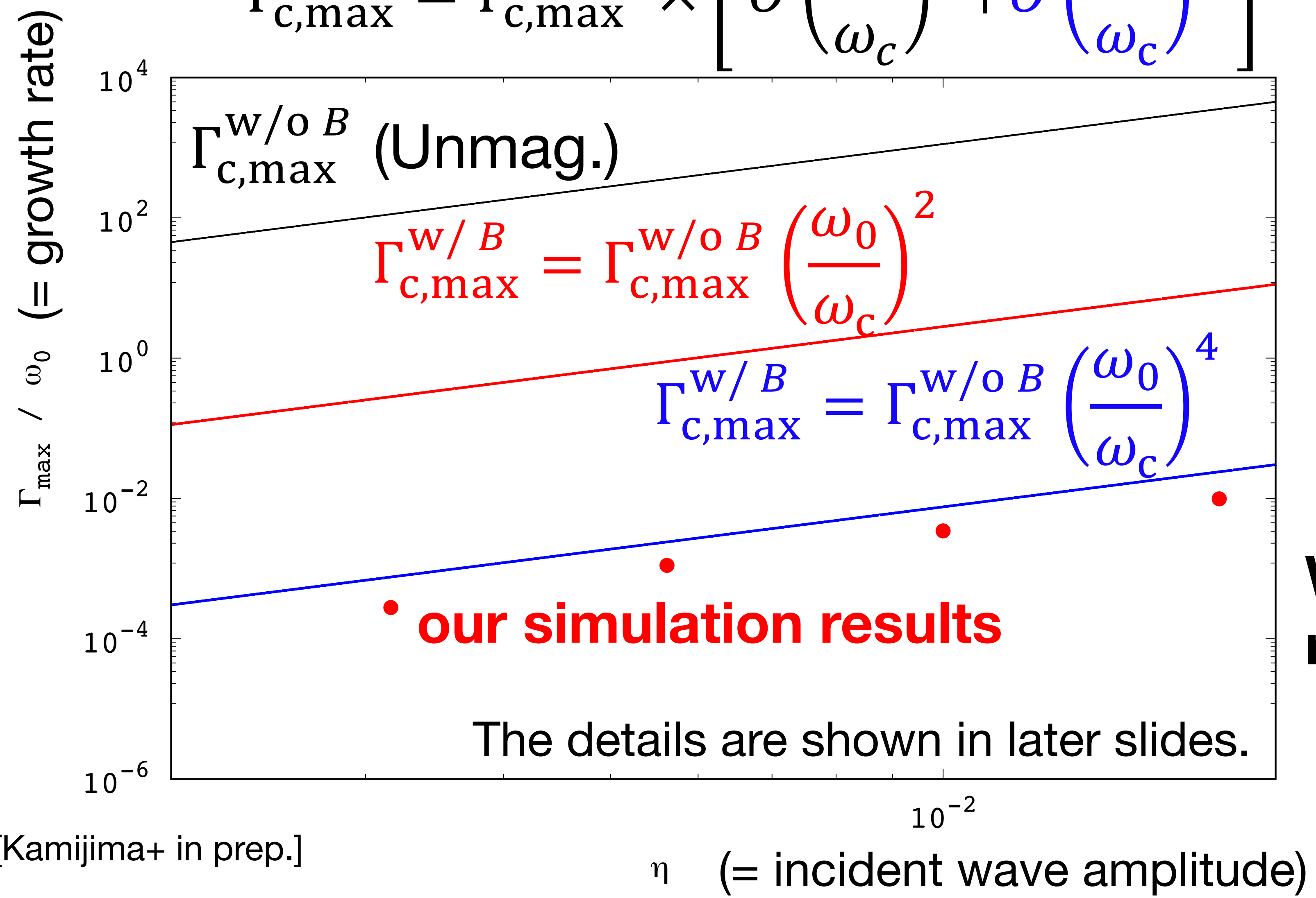

[Kamijima+ in prep.]

We reconsider the growth rate in magnetized plasma.

Parametric Instability in Magnetized Plasma

Particles oscillated by the incident wave make the nonlinear current.

↓

The nonlinear current generates the scattered wave.

↓

The beating wave between the incident and scattered waves is created.

↓

The ponderomotive force acts on particles.

↓

The density fluctuation is amplified.

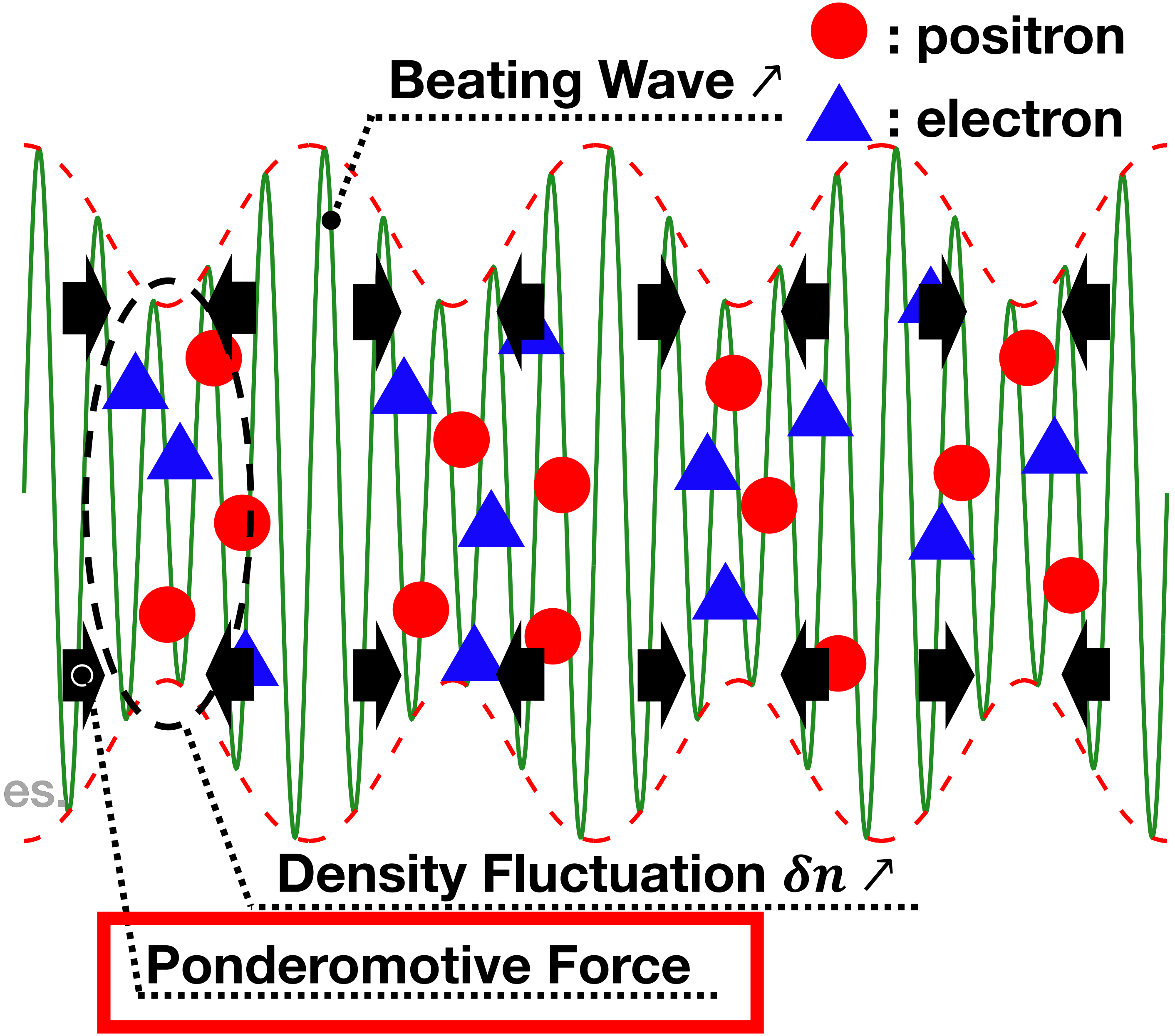

Ponderomotive Force in Magnetized Plasma

[e.g. Klima 1966, 1968, Lee & Parks 1983,1996]

$$\vec{F}_{\rm pond} = -\frac{e^2}{4m}\nabla\left[-\frac{|E_{\rm x}|^2+|E_{\rm z}|^2}{\omega_{\rm c}^2-\omega_0^2} \pm i\,\frac{\omega_{\rm c}(E_{\rm z}^*E_{\rm x}-E_x^*E_{\rm z})}{\omega_0(\omega_{\rm c}^2-\omega_0^2)}\right]$$

$+$: Positron
$-$: Electron

$\vec{B}_0, \vec{k}_0 \parallel y$

● : Positron

▲ : Electron

$\omega_{\rm c} = eB_0/(m_e c)$:cyclotron freq. > ω_0:incident wave freq.

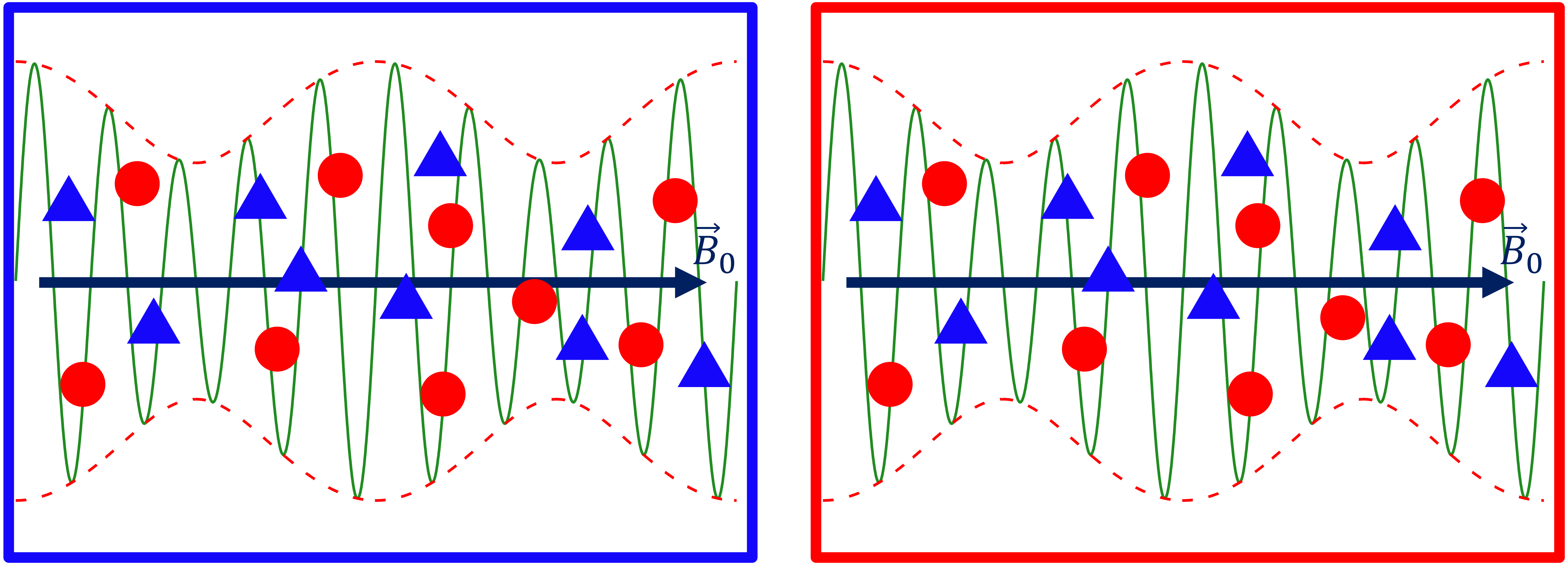

Growth Rate in Magnetized Plasma

[Nishiura & Ioka 2024, Nishiura+ in prep.]

$$\Gamma_{\mathrm{c,max}}^{\mathrm{w/}\ B} = \Gamma_{\mathrm{c,max}}^{\mathrm{w/o}\ B} \max\left[\left(\frac{\omega_0}{\omega_c}\right)^4, \frac{32\mathrm{e}}{\pi}\left(\frac{\omega_0}{\omega_\mathrm{c}}\right)^2\left(\frac{\omega_0}{\omega_\mathrm{p}}\right)^4\left(\frac{k_\mathrm{B}T_\mathrm{e}}{m_\mathrm{e}c^2}\right)^2\right]$$

Neutral Mode **Charged Mode**

● : **Positron**

▲ : **Electron** $\omega_\mathrm{c} = eB_0/(m_e c)$:cyclotron freq. > ω_p : plasma freq. > ω_0:incident wave freq.

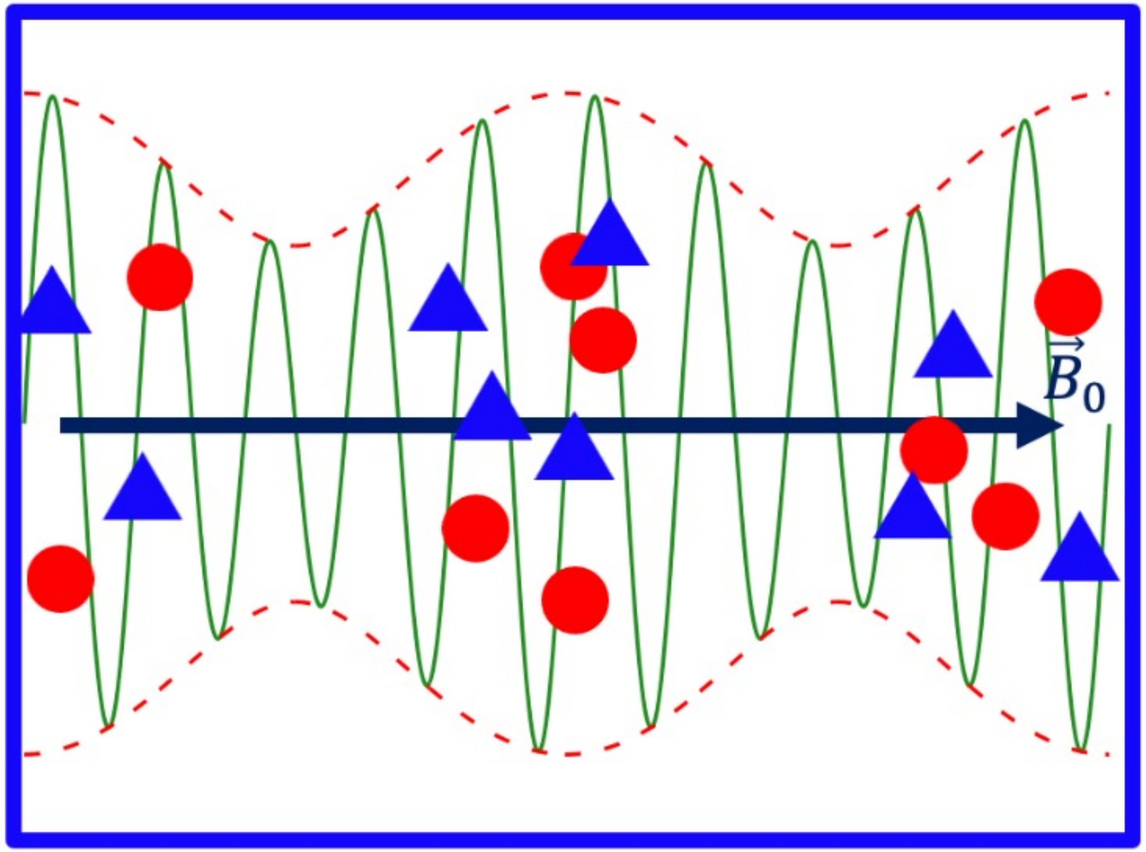

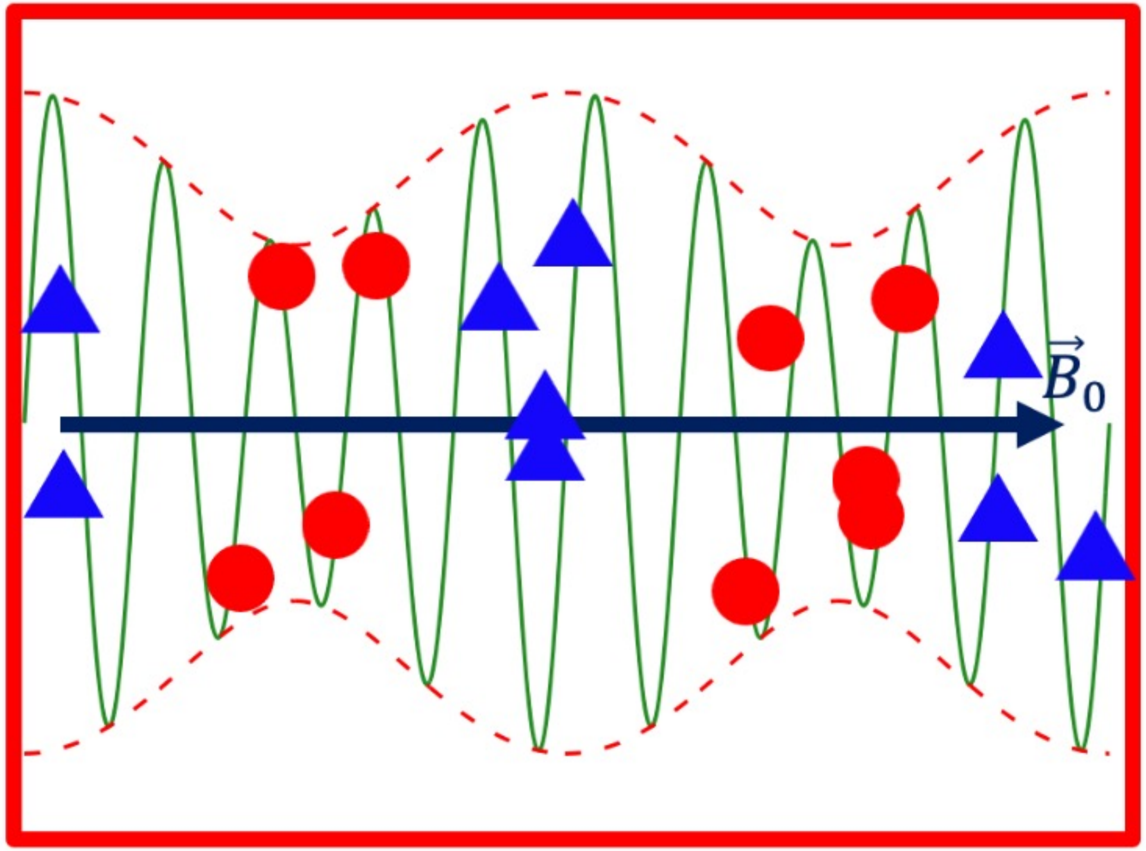

Growth Rate in Magnetized Plasma

[Nishiura & Ioka 2024, Nishiura+ in prep.]

Updated growth rate of ICS in magnetized plasma

$$\Gamma^{\mathrm{w/}\,B}_{\mathrm{c,max}} = \Gamma^{\mathrm{w/o}\,B}_{\mathrm{c,max}} \max\left[\left(\frac{\omega_0}{\omega_c}\right)^4, \frac{32\mathrm{e}}{\pi}\left(\frac{\omega_0}{\omega_c}\right)^2\left(\frac{\omega_0}{\omega_p}\right)^4\left(\frac{k_B T_e}{m_e c^2}\right)^2\right]$$

Neutral Mode — Charged Mode

We investigate the growth rate of neutral and charged modes by using Particle-in-Cell (PIC) simulations.

$$\omega_c > \omega_p > \omega_0$$

Particle-in-Cell (PIC) Simulation

- WumingPIC2D (public code) [Matsumoto+2024]
- Flow (Nagoya U.), Yukawa-21 (YITP), XC50 (CfCA)

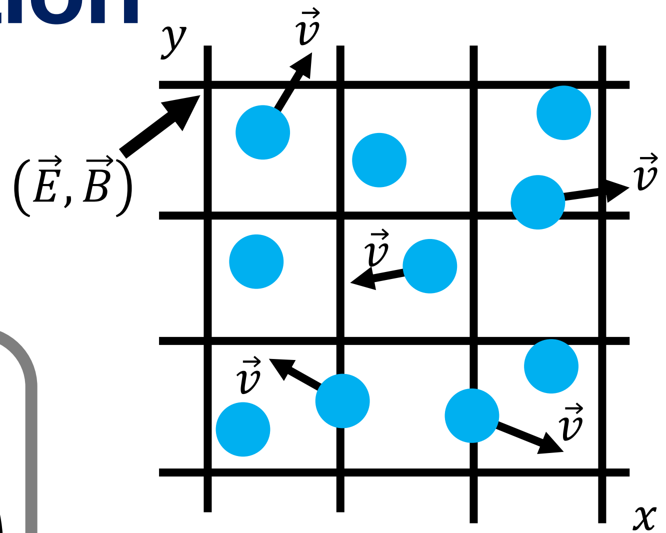

Solve EoM: $\vec{F} \rightarrow (\vec{x},\vec{v})$

$$\frac{d\vec{x}}{dt} = \vec{v}, \quad \frac{d(\gamma m\vec{v})}{dt} = \vec{F} = q\left(\vec{E} + \frac{\vec{v}}{c}\times\vec{B}\right)$$

Weighting
$(\vec{x},\vec{v}) \rightarrow (\rho,\vec{j})$

Δt

Solve Maxwell eqs.: $(\rho,\vec{j}) \rightarrow (\vec{E},\vec{B})$

$$\nabla\cdot\vec{E} = 4\pi\rho, \quad \nabla\cdot\vec{B} = 0$$

$$\nabla\times\vec{E} = -\frac{1}{c}\frac{\partial\vec{B}}{\partial t}, \quad \nabla\times\vec{B} = \frac{4\pi}{c}\vec{j} + \frac{1}{c}\frac{\partial\vec{E}}{\partial t}$$

Weighting
$(\vec{E},\vec{B}) \rightarrow \vec{F}$

Setup

Red values are given by hands.

$\Delta x = \Delta y = \Delta t = 1, m_e = 1, c = 1$

- mass ratio: $m_r = m_i/m_e = 1$ (e± plasma)
- ratio of incident wave freq. (ω_0) & plamsa freq. (ω_{pe})

$$\frac{\omega_0}{\omega_{pe}} = 0.1, 0.9 \quad \left(\omega_0 \Delta t < \omega_{pe} \Delta t < \omega_c \Delta t = \sqrt{\sigma_e}\,\omega_{pe} \Delta t < 0.1\right)$$

- electron sigma parameter:

$$\sigma_e = \frac{B_0^2}{4\pi n_e m_e c^2} = 4, 10000$$

- thermal velocities of e± plasma

$$\frac{v_{th,e}}{c} = \sqrt{\frac{k_B T_e}{m_e c^2}} = \frac{v_{th,i}}{c} = 0.03, 0.5$$

- ratio of incident wave amp.(B_p) & background B-field (B_0)

$$\eta = \frac{B_p}{B_0} \approx 0.0031 - 0.56$$

- The number of particles in each cell

$$n = 100\ /\text{cell}$$

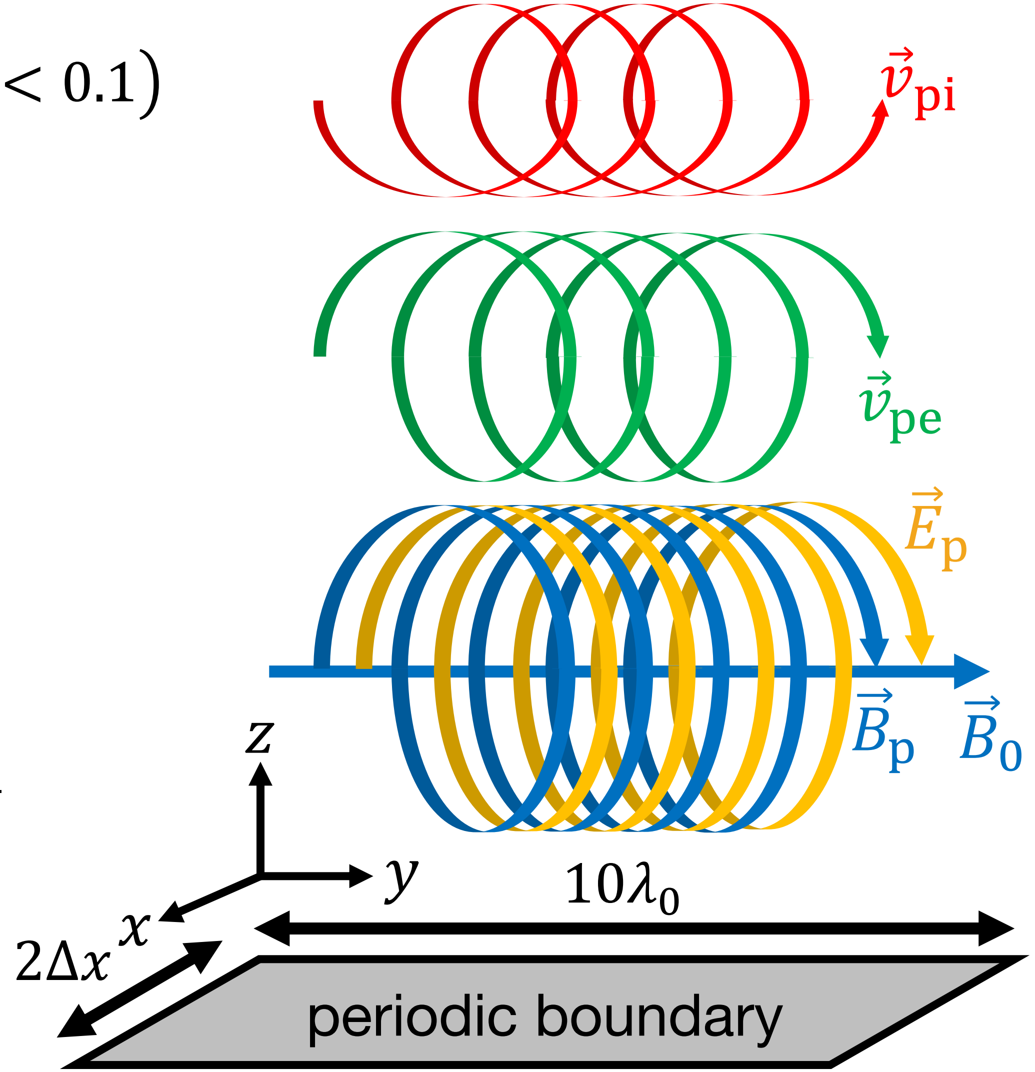

Setup

Red values are given by hands.

$$\Delta x = \Delta y = \Delta t = 1, m_e = 1, c = 1$$

- Right-handed circular pol. Alfvén wave (incident wave)

[Matsukiyo & Hada 2003]

$$\vec{B}_p = B_p[-\sin\phi_0\,\hat{x} + \cos\phi_0\,\hat{z}], \phi_0 = k_0 y - \omega_0 t$$

$$\vec{E}_p = -\frac{\omega_0}{ck_0} B_p[\cos\phi_0\,\hat{x} + \sin\phi_0\,\hat{z}] \qquad \eta = B_p/B_0$$

$$\left(\frac{ck_0}{\omega_0}\right)^2 = 1 - \frac{\omega_{pe}^2}{\omega_0(\gamma_e\omega_0 - \omega_c)} - \frac{\omega_{pi}^2}{\omega_0(\gamma_i\omega_0 + \omega_c)}$$

- initial e± plasma velocity

$$\frac{\vec{v}_e}{c} = \frac{\omega_0}{ck_0}\frac{\eta\omega_c}{\gamma_e\omega_0 - \omega_c}\frac{\vec{B}_p}{B_p} \qquad \frac{\vec{v}_i}{c} = -\frac{\omega_0}{ck_0}\frac{\eta\omega_c}{\gamma_i\omega_0 + \omega_c}\frac{\vec{B}_p}{B_p}$$

$$\gamma_{e(i)} = \frac{1}{\sqrt{1 - \left(\frac{v_{e(i)}}{c}\right)^2}}$$

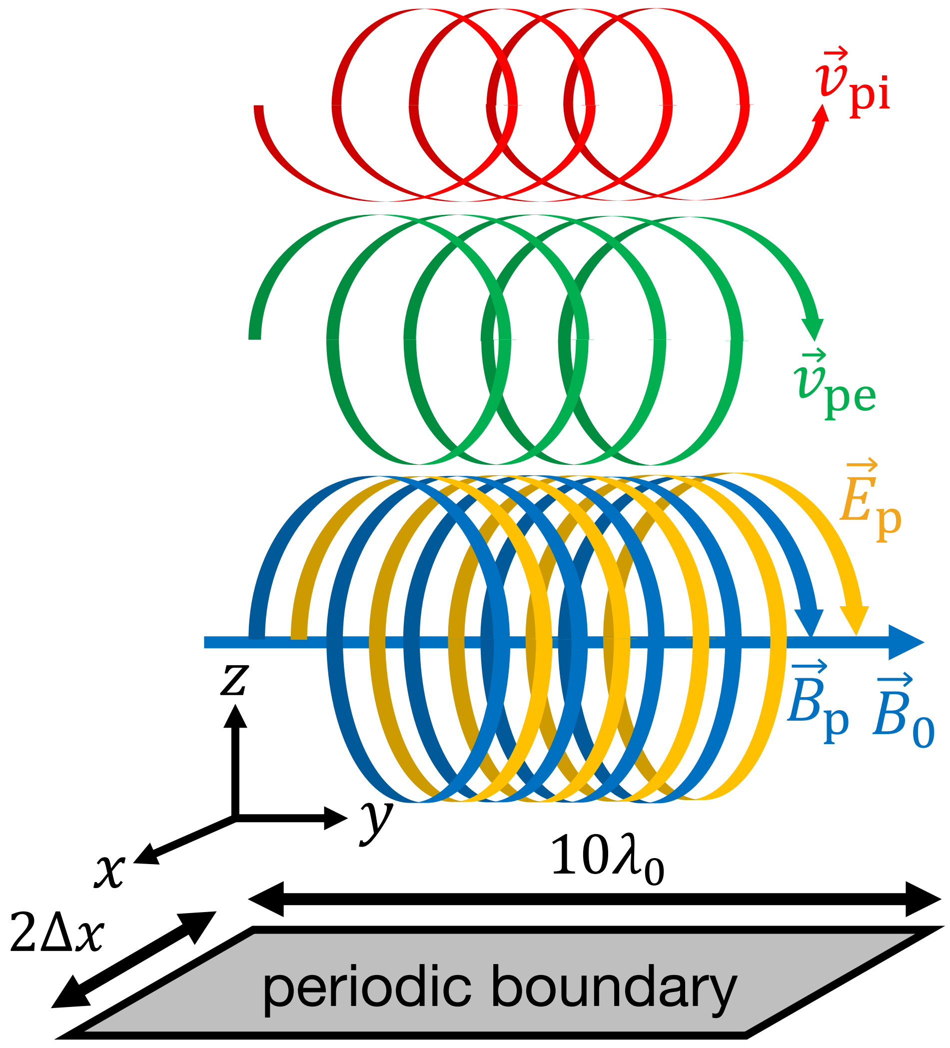

Wave Decomposition

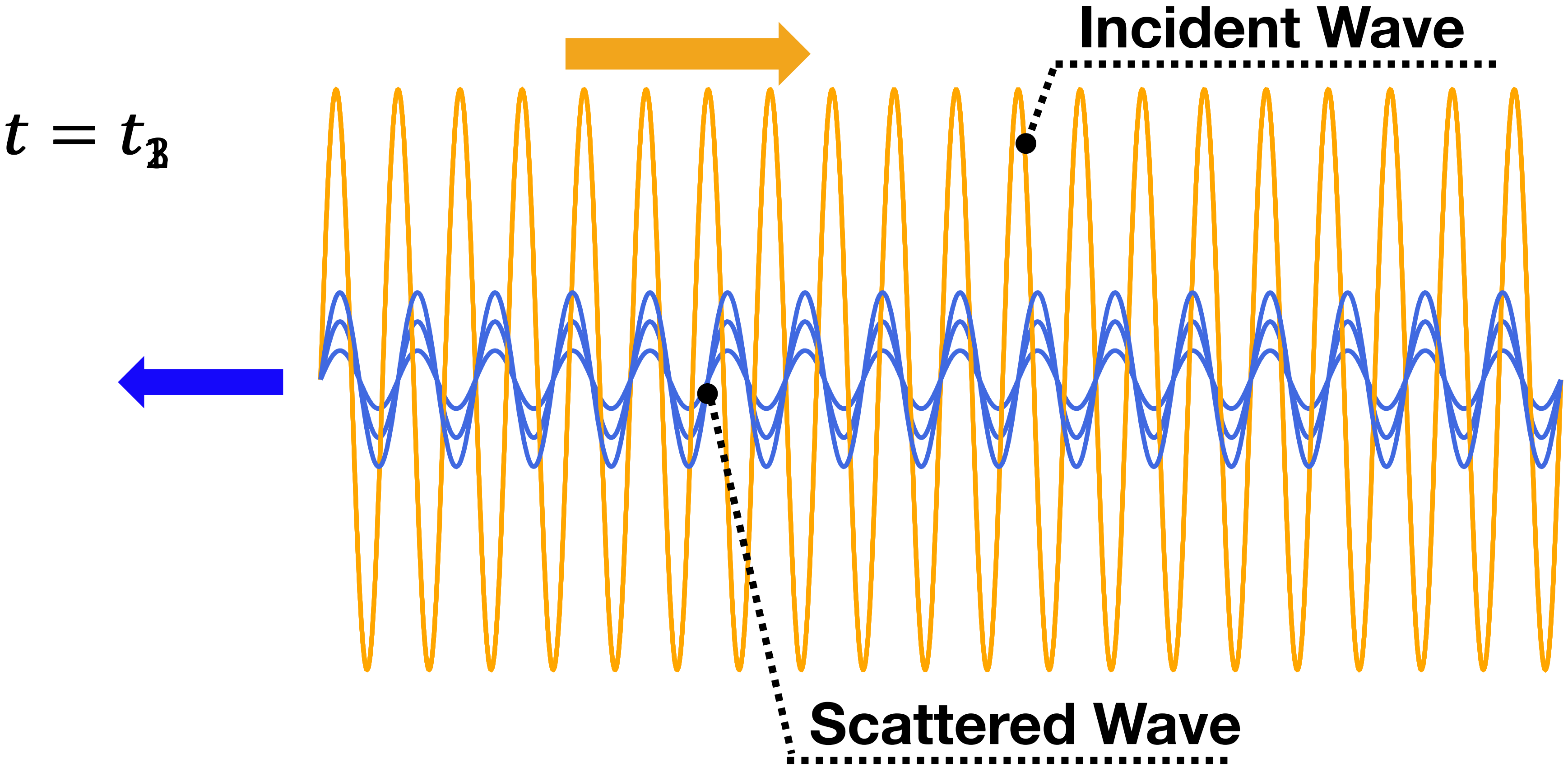

The growth rate is estimated from the time evolution of the power (or amplitude) of the scattered wave.

We decompose the forward propagating incident wave and the backward propagating scattered wave from the snapshot data.

Results

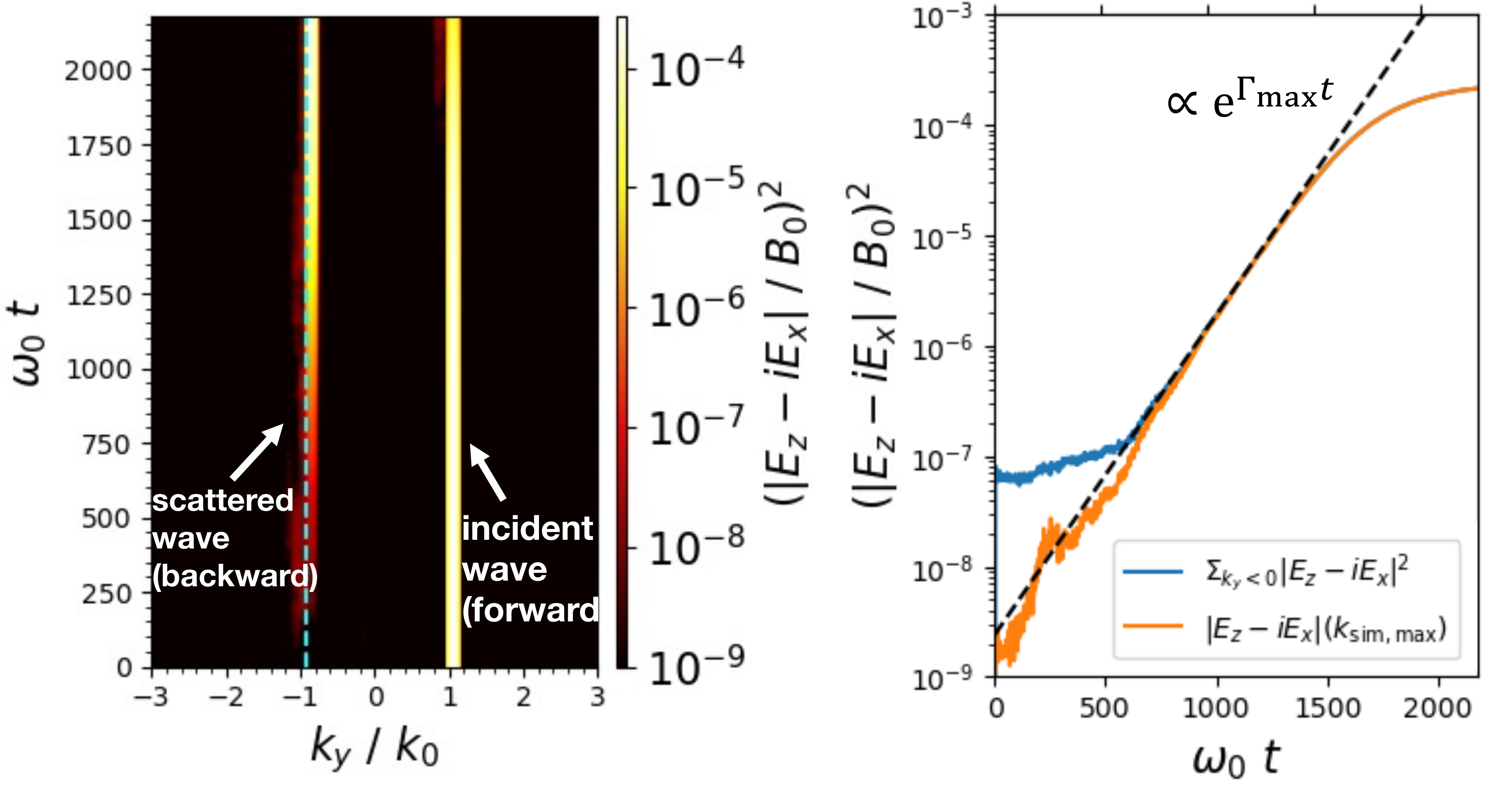
scattered wave (backward)
incident wave (forward)
$\omega_0\, t$
$k_y\ /\ k_0$
$(|E_z - iE_x|\ /\ B_0)^2$
$\propto e^{\Gamma_{\max} t}$
$\Sigma_{k_y<0}|E_z - iE_x|^2$
$|E_z - iE_x|(k_{\mathrm{sim,\,max}})$

Charged Mode

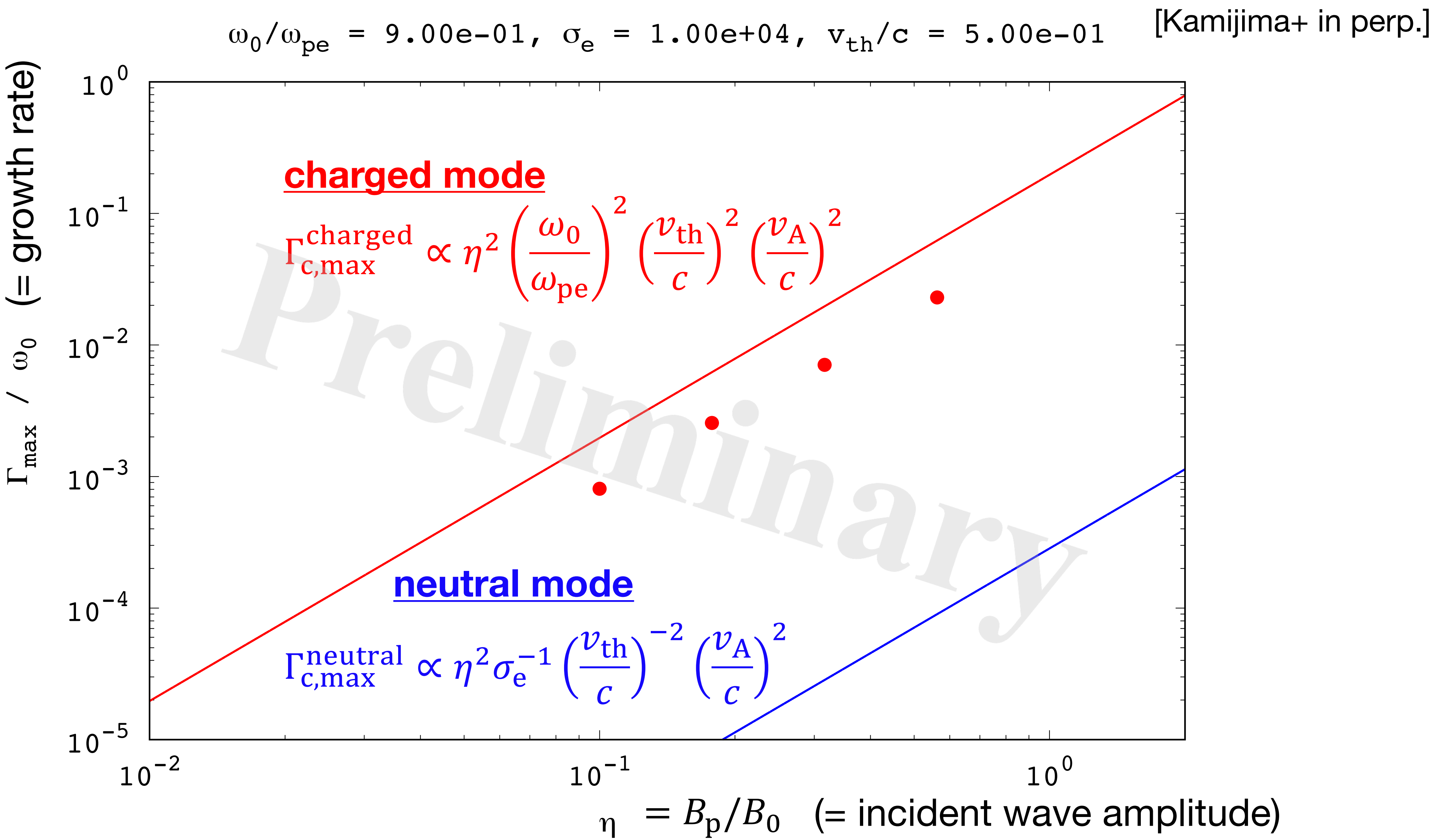

Charged Mode

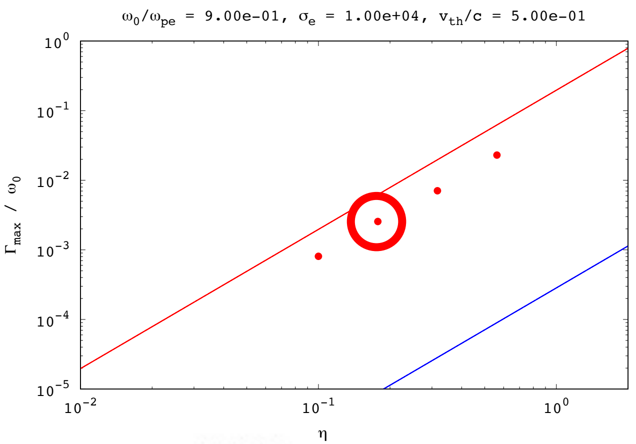

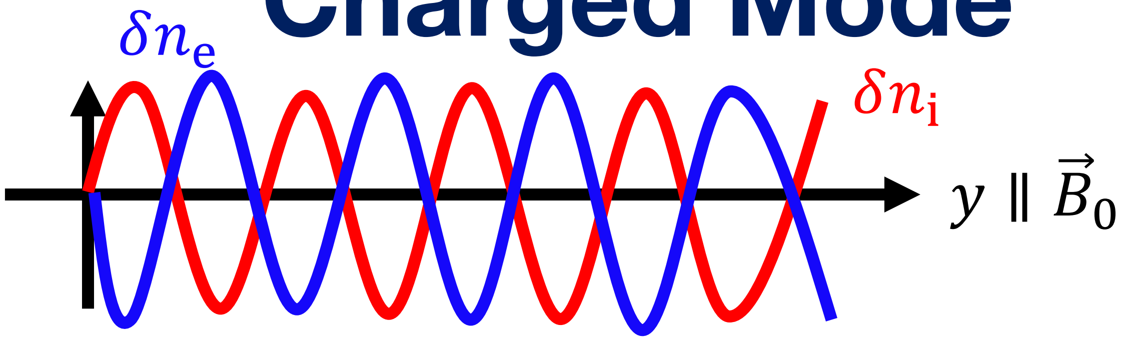

$\delta n_i + \delta n_e \xrightarrow{FT}$ **vanish**

$\delta n_i - \delta n_e \rightarrow$ **remain**

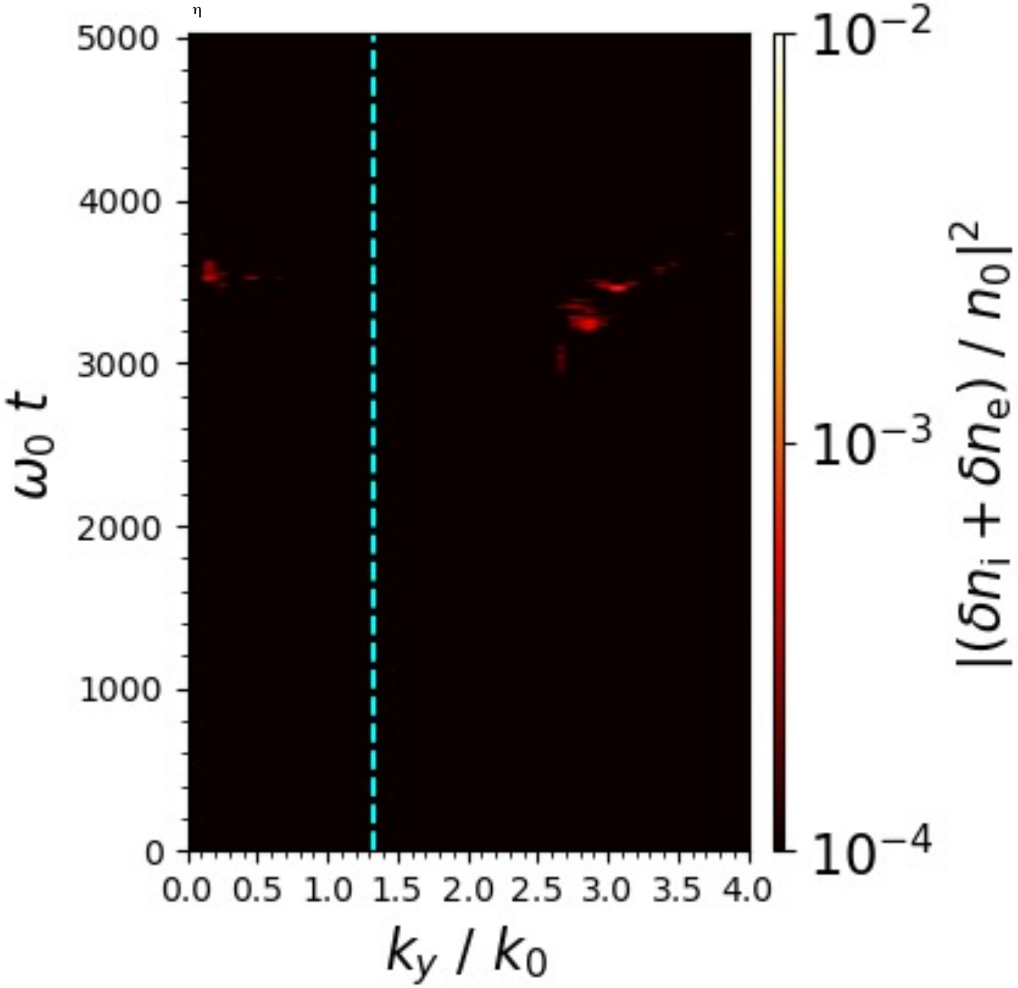

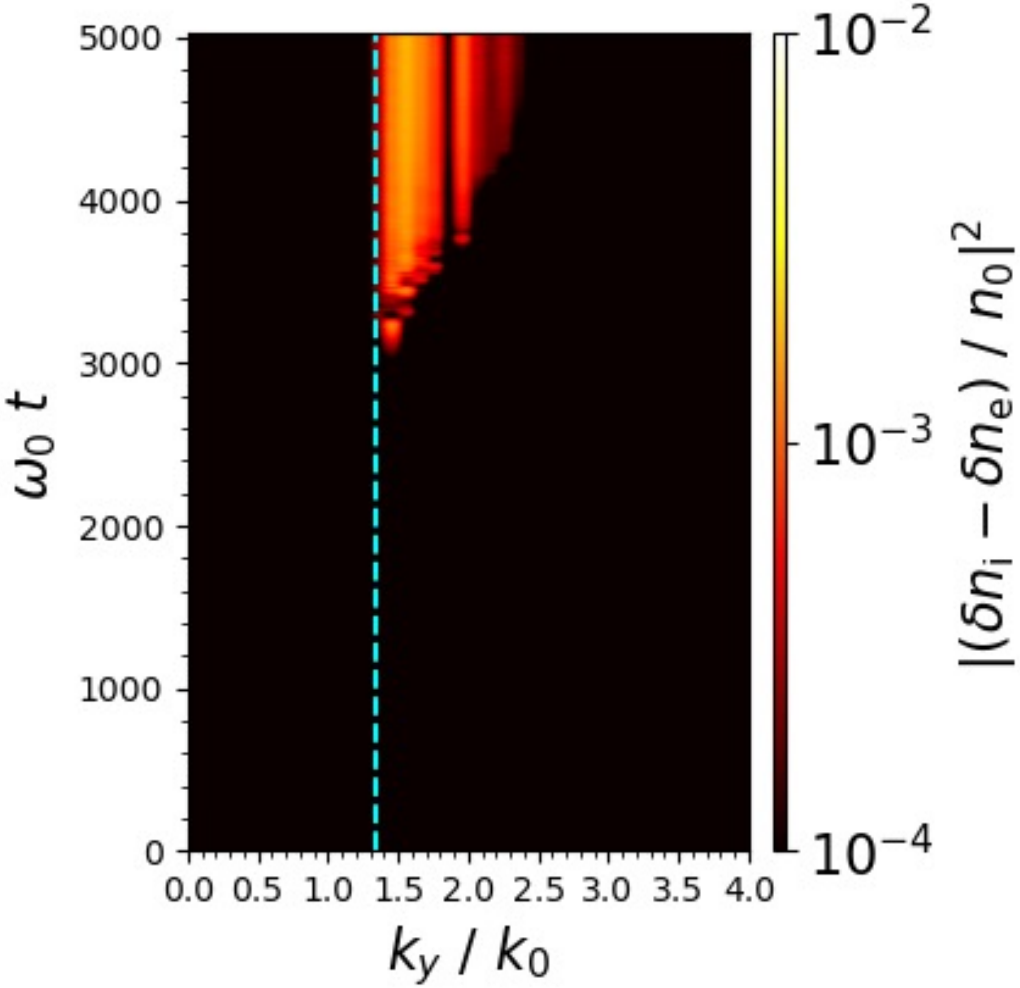

Charged Mode

[Kamijima+ in perp.]

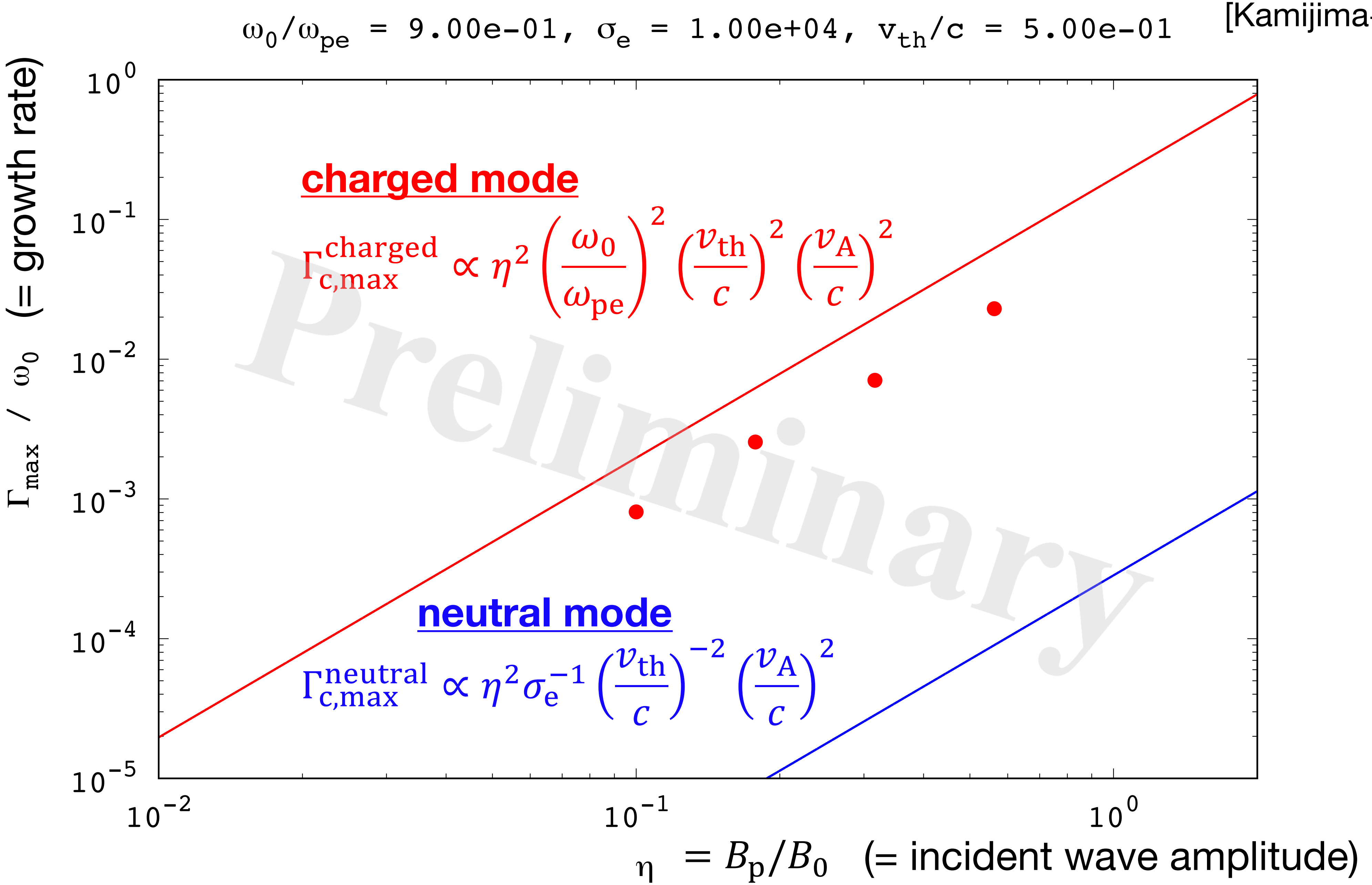

Neutral Mode

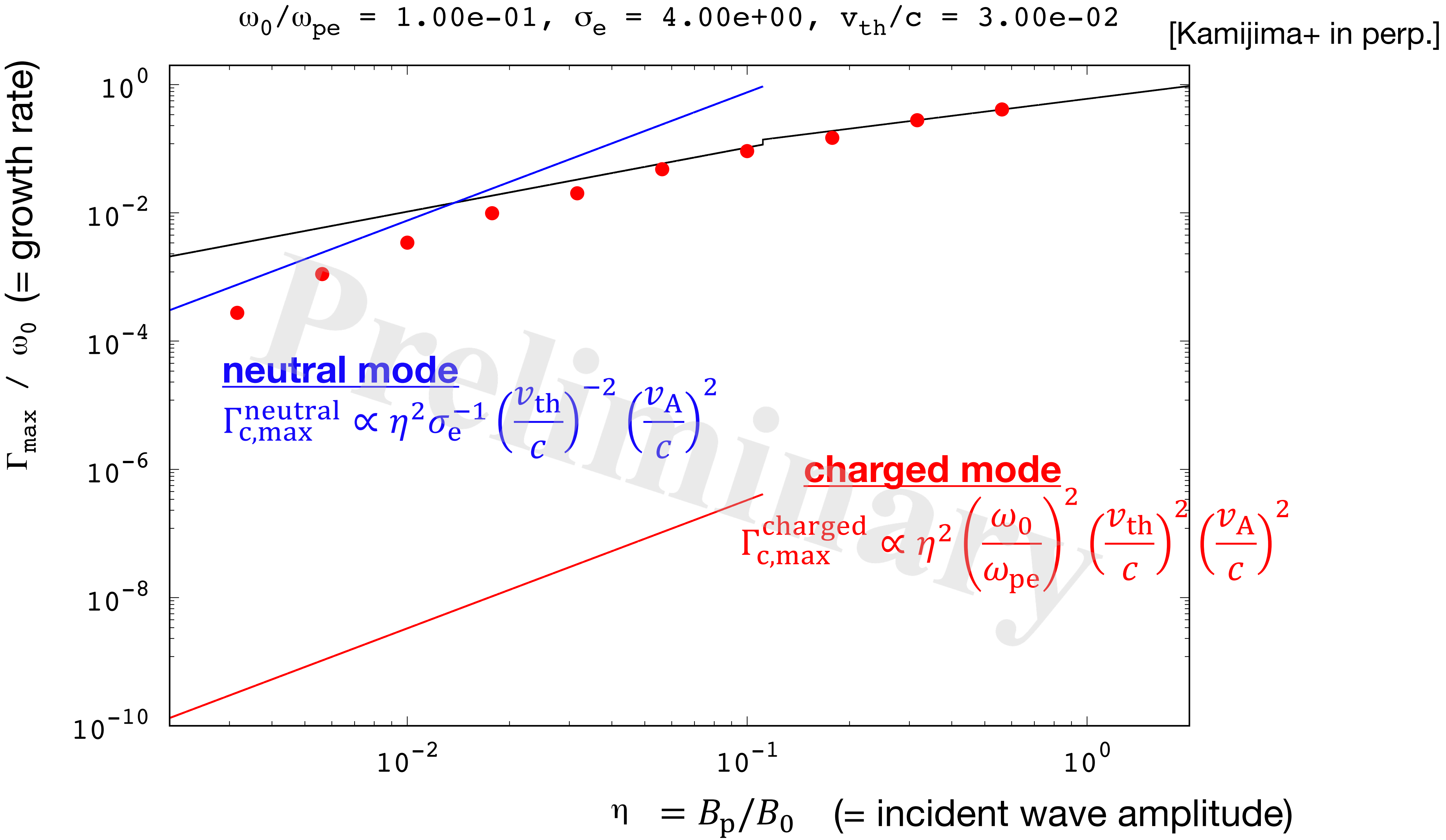

Neutral Mode

[Kamijima+ in perp.]

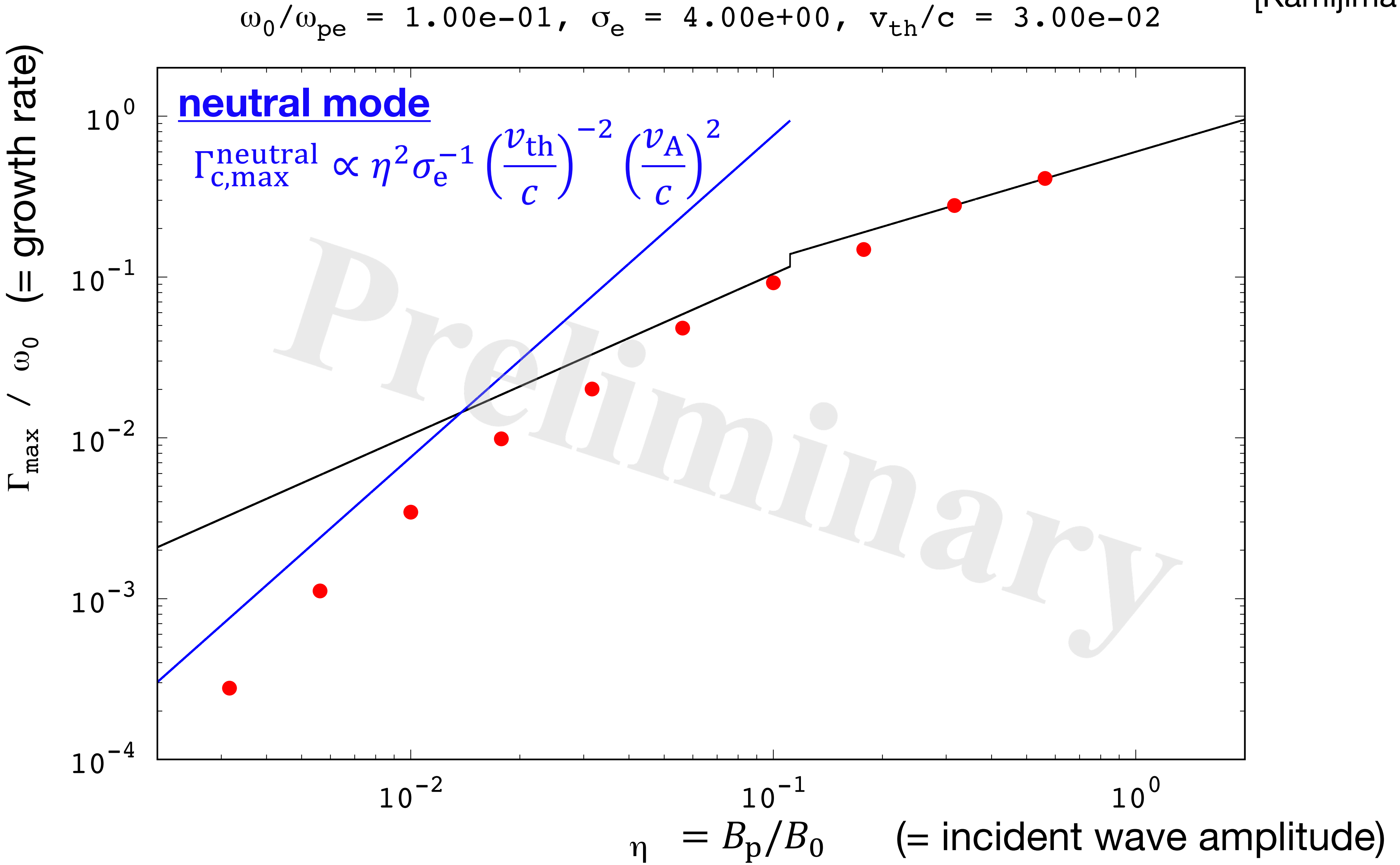

Neutral Mode

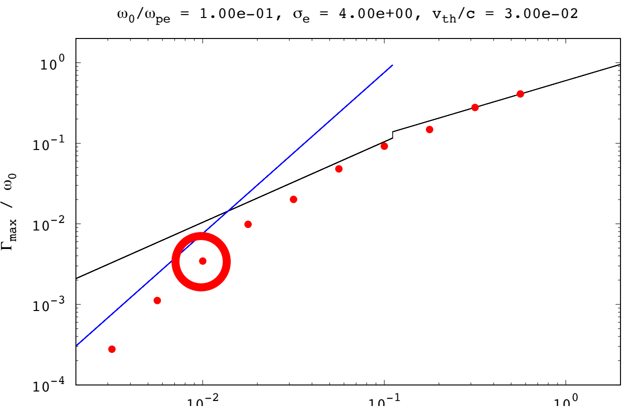

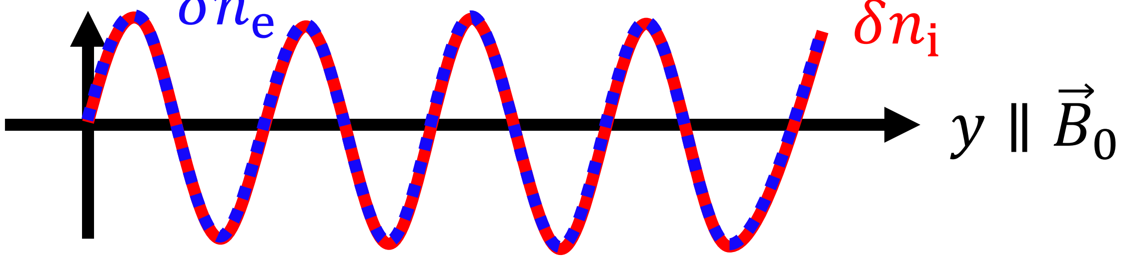

FT

$\delta n_i + \delta n_e$ → **remain**

$\delta n_i - \delta n_e$ → **vanish**

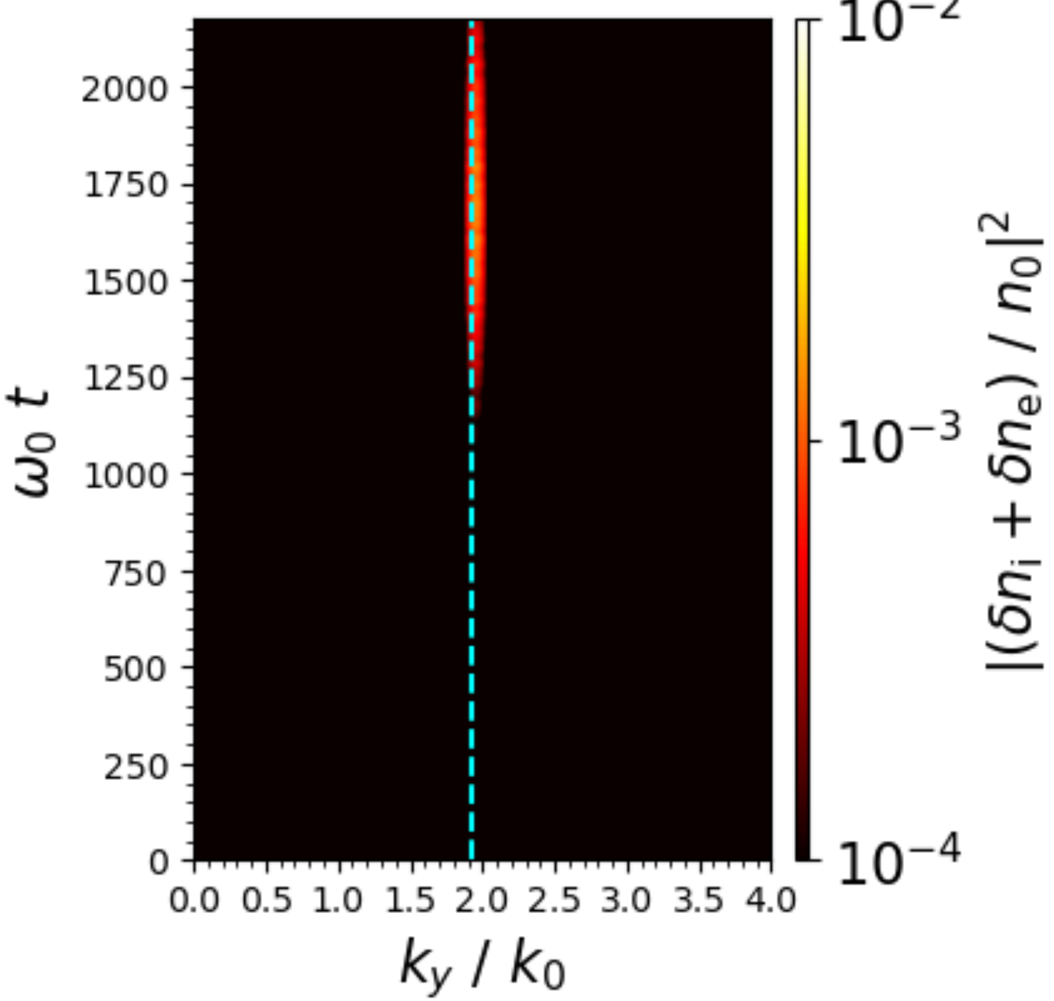

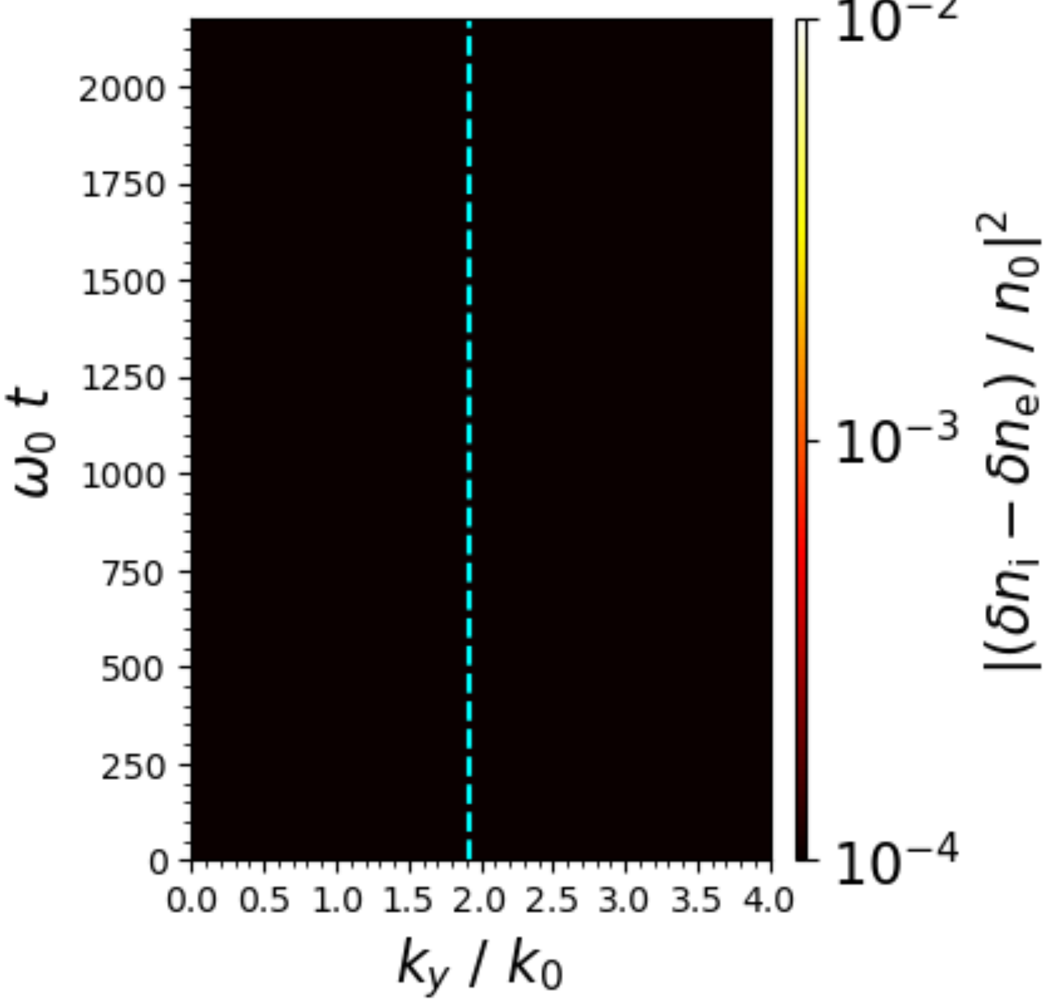

Neutral Mode vs. Induced Brillouin Scattering

[Kamijima+ in perp.]

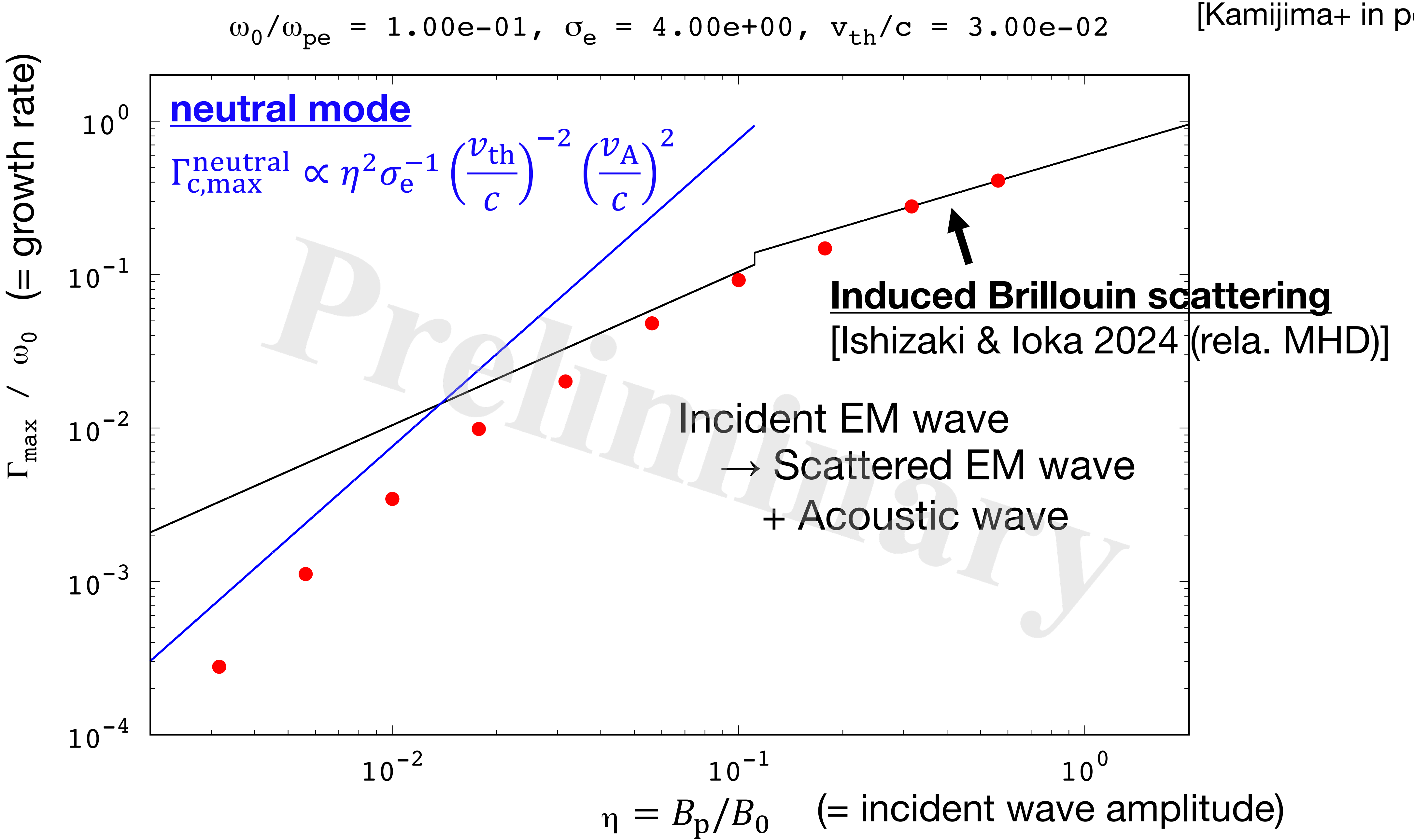

Neutral Mode vs. Induced Brillouin Scattering

[Kamijima+ in perp.]

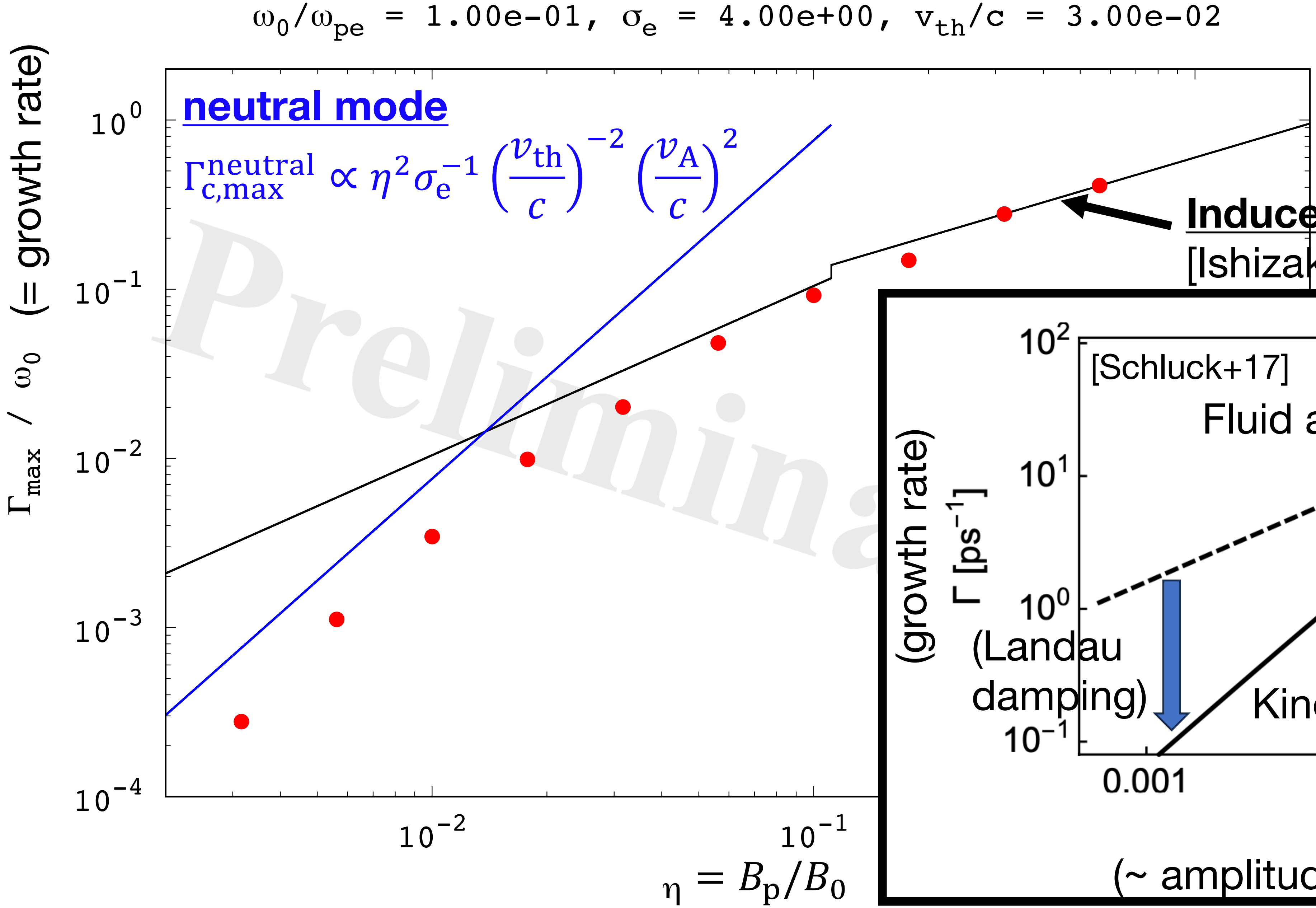

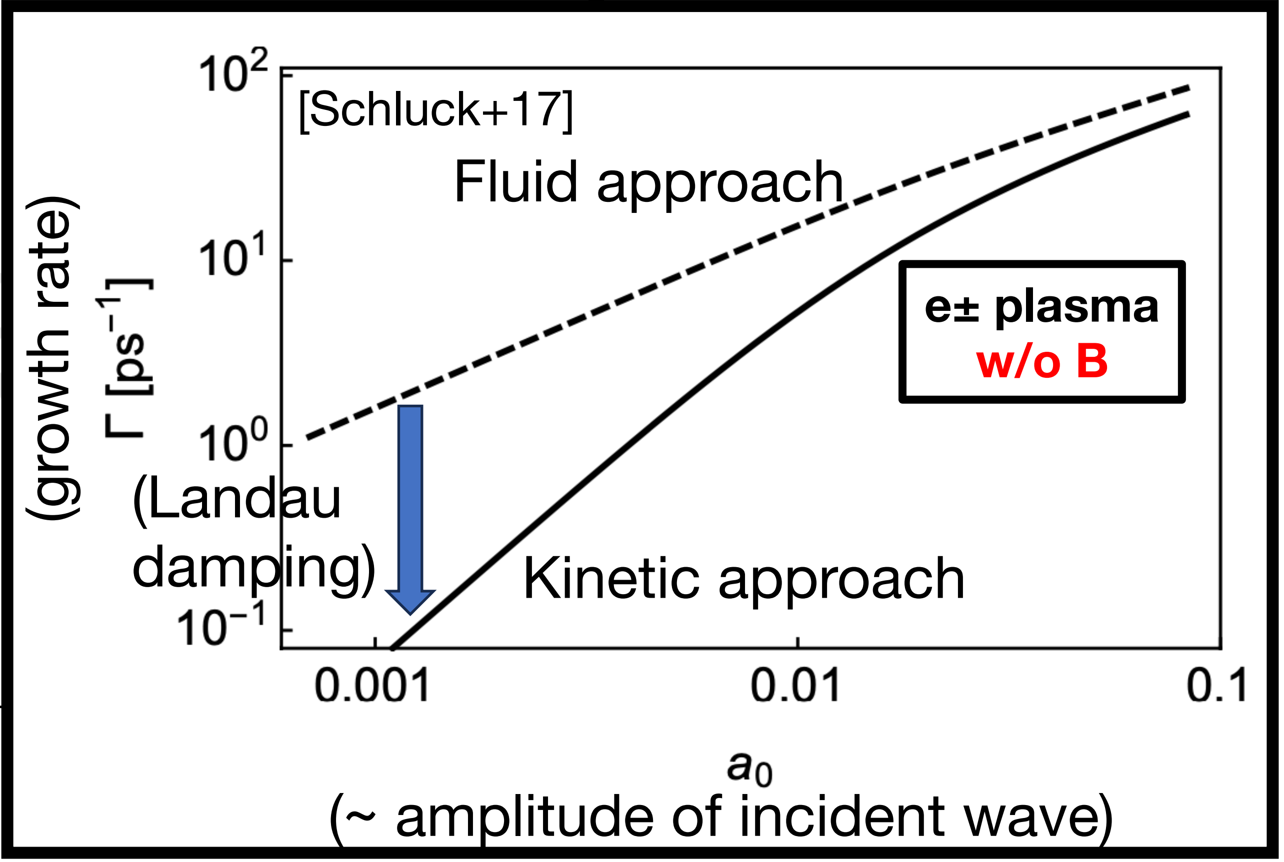

Summary & Future Work

- We investigate propagation of Alfvén waves in magnetized pair plasma by using Particle-in-Cell simulations.

- Simulation results are almost in good agreement with the theoretical growth rate of induced Compton scatterings (charged & neutral modes) and induced Brillouin scatterings.

- Incident wave: plane wave -> pulse, circular pol. -> linear pol.

- Nonlinear phase & Saturation

- Dependency of other parameters.